http://www.icact.org/journal.asp

ICACT-TACT JOURNAL

Transactions on Advanced Communications Technology

Volume 6 Issue 1, Jan. 2017, ISSN: 2288-0003

Editor-in-Chief
Prof. Thomas Byeongnam YOON, PhD.

Global IT Research Institute

Journal Editorial Board

Editor Guide

■ Introduction for Editor or Reviewer

All the editor group members are to be assigned as a evaluator(editor or reviewer) to submitted journal papers at the discretion of the Editor-in-Chief. It will be informed by eMail with a Member Login ID and Password.

Once logined the Website via the Member Login menu in left as a evaluator, you can find out the paper assigned to you. You can evaluate it there. All the results of the evaluation are supposed to be shown in the Author Homepage in the real time manner. You can also enter the Author Homepage assigned to you by the Paper ID and the author's eMail address shown in your Evaluation Webpage. In the Author Homepage, you can communicate each other efficiently under the peer review policy. Please don't miss it!

All the editor group members are supposed to be candidates of a part of the editorial board, depending on their contribution which comes from history of ICACT TACT as an active evaluator. Because the main contribution comes from sincere paper reviewing role.

■ Role of the Editor

The editor's primary responsibilities are to conduct the peer review process, and check the final camera-ready manuscripts for any technical, grammatical or typographical errors.

As a member of the editorial board of the publication, the editor is responsible for ensuring that the publication maintains the highest quality while adhering to the publication policies and procedures of the ICACT TACT(Transactions on the Advanced Communications Technology).

For each paper that the editor-in-chief gets assigned, the Secretariat of ICACT Journal will send the editor an eMail requesting the review process of the paper.

The editor is responsible to make a decision on an "accept", "reject", or "revision" to the Editor-in-Chief via the Evaluation Webpage that can be shown in the Author Homepage also.

■ Deadlines for Regular Review

Editor-in-Chief will assign a evalaution group(a Editor and 2 reviewers) in a week upon receiving a completed Journal paper submission. Evaluators are given 2 weeks to review the paper. Editors are given a week to submit a recommendation to the Editor-in-Chief via the evaluation Webpage, once all or enough of the reviews have come in. In revision case, authors have a maximum of a month to submit their revised manuscripts. The deadlines for the regular review process are as follows:

Evalution Procedure	Deadline
Selection of Evaluation Group	1 week
Review processing	2 weeks
Editor's recommendation	1 week
Final Decision Noticing	1 week

■ Making Decisions on Manuscript

Editor will make a decision on the disposition of the manuscript, based on remarks of the reviewers. The editor's recommendation must be well justified and explained in detail. In cases where the revision is requested, these should be clearly indicated and explained. The editor must then promptly convey this decision to the author. The author may contact the editor if instructions regarding amendments to the manuscript are unclear. All these actions could be done via the evaluation system in this Website. The guidelines of decisions for publication are as follows:

Decision	Description
Accept	An accept decision means that an editor is accepting the paper with no further modifications. The paper will not be seen again by the editor or by the reviewers.
Reject	The manuscript is not suitable for the ICACT TACT publication.
Revision	The paper is conditionally accepted with some requirements. A revision means that the paper should go back to the original reviewers for a second round of reviews. We strongly discourage editors from making a decision based on their own review of the manuscript if a revision had been previously required.

■ Role of the Reviewer

Reviewer Webpage:

Once logined the Member Login menu in left, you can find out papers assigned to you. You can also login the Author Homepage assigned to you with the paper ID and author's eMail address. In there you can communicate each other via a Communication Channel Box.

Quick Review Required:

You are given 2 weeks for the first round of review and 1 week for the second round of review. You must agree that time is so important for the rapidly changing IT technologies and applications trend. Please respect the deadline. Authors undoubtedly appreciate your quick review.

Anonymity:

Do not identify yourself or your organization within the review text.

Review:

Reviewer will perform the paper review based on the main criteria provided below. Please provide detailed public comments for each criterion, also available to the author.

- How this manuscript advances this field of research and/or contributes something new to the literature?
- Relevance of this manuscript to the readers of TACT?
- Is the manuscript technically sound?
- Is the paper clearly written and well organized?
- Are all figures and tables appropriately provided and are their resolution good quality?
- Does the introduction state the objectives of the manuscript encouraging the reader to read on?
- Are the references relevant and complete?

Supply missing references:

Please supply any information that you think will be useful to the author in revision for enhancing quality of the paperor for convincing him/her of the mistakes.

Review Comments:

If you find any already known results related to the manuscript, please give references to earlier papers which contain these or similar results. If the reasoning is incorrect or ambiguous, please indicate specifically where and why. If you would like to suggest that the paper be rewritten, give specific suggestions regarding which parts of the paper should be deleted, added or modified, and please indicate how.

Journal Procedure

Dear Author,

- **You can see all your paper information & progress.**

- **Step 1. Journal Full Paper Submission**

Using the Submit button, submit your journal paper through ICACT Website, then you will get new paper ID of your journal, and send your journal Paper ID to the Secretariat@icact.org for the review and editorial processing. Once you got your Journal paper ID, never submit again! Journal Paper/CRF Template

- **Step 2. Full Paper Review**

Using the evaluation system in the ICACT Website, the editor, reviewer and author can communicate each other for the good quality publication. It may take about 1 month.

- **Step 3. Acceptance Notification**

It officially informs acceptance, revision, or reject of submitted full paper after the full paper review process.

Status	Action
Acceptance	Go to next Step.
Revision	Re-submit Full Paper within 1 month after Revision Notification.
Reject	Drop everything.

- **Step 4. Payment Registration**

So far it's free of charge in case of the journal promotion paper from the registered ICACT conference paper! But you have to regist it, because you need your Journal Paper Registration ID for submission of the final CRF manuscripts in the next step's process. Once you get your Registration ID, send it to Secretariat@icact.org for further process.

- **Step 5. Camera Ready Form (CRF) Manuscripts Submission**

After you have received the confirmation notice from secretariat of ICACT, and then you are allowed to submit the final CRF manuscripts in PDF file form, the full paper and the Copyright Transfer Agreement. Journal Paper Template, Copyright Form Template, BioAbstract Template,

Journal Submission Guide

All the Out-Standing ICACT conference papers have been invited to this "ICACT Transactions on the Advanced Communications Technology" Journal, and also welcome all the authors whose conference paper has been accepted by the ICACT Technical Program Committee, if you could extend new contents at least 30% more than pure content of your conference paper. Journal paper must be followed to ensure full compliance with the IEEE Journal Template Form attached on this page.

➢ How to submit your Journal paper and check the progress?

Step 1. Submit	Using the Submit button, submit your journal paper through ICACT Website, then you will get new paper ID of your journal, and send your journal Paper ID to the Secretariat@icact.org for the review and editorial processing. Once you got your Journal paper ID, never submit again! Using the Update button, you can change any information of journal paper related or upload new full journal paper.
Step 2. Confirm	Secretariat is supposed to confirm all the necessary conditions of your journal paper to make it ready to review. In case of promotion from the conference paper to Journal paper, send us all the .DOC(or Latex) files of your ICACT conference paper and journal paper to evaluate the difference of the pure contents in between at least 30% more to avoid the self replication violation under scrutiny. The pure content does not include any reference list, acknowledgement, Appendix and author biography information.
Step 3. Review	Upon completing the confirmation, it gets started the review process thru the Editor & Reviewer Guideline. Whenever you visit the Author Homepage, you can check the progress status of your paper there from start to end like this, " Confirm OK! -> Gets started the review process -> ...", in the Review Status column. Please don't miss it!

Volume. 6 Issue. 1

A Process-Aware Goal Description Language for the Internet of Things Community Computing Environments

Hyunah Kim*, Kwanghoon Pio Kim*
*Dept. of Computer Science, KYONGGI UNIVERSITY, Suwonsi Kyonggido, Republic of Korea
hyuna2486@naver.com, kwang@kgu.ac.kr

***Abstract*—This paper proposes an abstract language for describing process-aware goals to be accomplished by collaborative smart-objects communities over the Internet of Things (IoT) platforms. The proposed abstract language is based upon the process-driven IoT-community computing model [1] that is derived from a conceptual integration of the process-aware collaborations and the standardized IoT framework announced *via* the ITU-T SG13[1] Y.2060. We assume that a group of collaborative smart-objects communities can be built-up statically, dynamically, or autonomously and their process-aware goals can be specified and achieved adaptively over an IoT-based community computing environment. We also strongly expect that the proposed abstract language will deliver us a meaningful means in specifying and achieving adaptive process-aware goals of the IoT-based communities formed in a ubiquitous computing society.**

***Keywords*-community computing model, the Internet of Things, Web of Things, smart-objects collaboration, process-aware goal description language, ubiquitous community computing architectures and systems**

I. Introduction

In recent, we are in the midmost era of the Internet of Things[2], which provides a variety of smart-objects collaboration services on ubiquitous computing environments. The widespread use of mobile smart-phones, smart-watches and O2O[2] products is the evident, and these little gadgets have become an integral and intimate part of everyday life for many millions of people, even more than the internet users. According to the report of [2], this situation opened a new form of communication between people and things, and between things themselves, which means that a new dimension, *anything* connectivity, has been emerging in the world of information and communications technologies characterized with *anytime* connectivity and *anyplace* connectivity for anyone. These three dimensions (*anything*, *anytime*, and *anyplace*) of connectivity give a clue to creating an entirely new dynamic network of networks—the Internet of Things (IoT)—as a future network.

The Internet of Things (which is abbreviated as IoT) is a conceptual platform for the ubiquitous community computing environments[3], and it is conceptually widened into the Web of Things (WoT)[4] and the Web of Objects (WoO), which have been recently issued in the RFID and sensor network (USN) literature. The IoT-based community computing environment supports the concept of ubiquitous community and society computing models and systems[3], and physically implies a computerized situation or space formed by a group of smart objects (or Things)[5], such as devices, sensors, actuators, and people as well, each of which may have various computing capabilities and/or ubiquitous networking capabilities. In the previous research of the authors' research group, we proposed an advanced and new community computing concept, which is called process-driven community computing model[1], with aiming to be deployed on the IoT-based community computing environment.

Imagine that a group of community-members (smart objects or Things) on an IoT-based community conducts their own roles to accomplish the community's goal in a fashion of process-aware collaborations[6][7]. For the sake of realizing the imagination, we tried to extend the ITU's standardized IoT framework by embedding the concept of process-aware collaborations into the standardized IoT conceptual architecture. As the next step of the research work, this paper devises an XML-based abstract language to describe a process-aware goal that should be accomplished by an IoT-based community over the Internet of Things community computing environment. The XML-based abstract language is called a process-aware goal description language that is based upon a set of XML-based schema structures consisting of procedural combinations of atomic role types[8] and compound role types[8], such as DAG (Directed Acyclic Graph) role, IF role, FOR role, WHILE role, and ALT (alternative) role.

II. Process-Aware IoT Communities

In this subsection, we introduce a conceptual definition of process-aware communities on the Internet of Things community computing environment. The IoT community computing environment is a computerized situation and society where a group of Things, including smart objects like devices, sensors, actuators, and even people, is connected each other through the Internet, and a partial group of the members is organized into a collaborative community (statically, dynamically, or

---

Manuscript received October 31, 2016. This work is a follow up of the accepted conference paper as an outstanding paper in the 18th IEEE International Conference on Advanced Communications Technology.

Hyunah Kim is with the department of computer science, Kyonggi University, 154-42 Kwangkyosan-ro Youngtong-gu Suwon-si Gyeonggi-do, 16227, Republic of Korea (e-mail: hyuna2486@naver.com)

Kwanghoon Pio Kim is with the collaboration technology research laboratory in the department of computer science, Kyonggi University, 154-42 Kwangkyosan-ro Youngtong-gu Suwon-si Gyeonggi-do, 16227, Republic of Korea (correponding author, phone: +82-31-249-9679, fax: +82-31-249-8949, e-mail: kwang@kgu.ac.kr)

[1]International Telecommunication Union, Telecommunication Standardization Sector, Study Group 13 - Future Networks

[2]O2O stands for Online-To-Offline combining the online shopping and the front line transactions, and it represents a recent IT convergence business model and its related products.

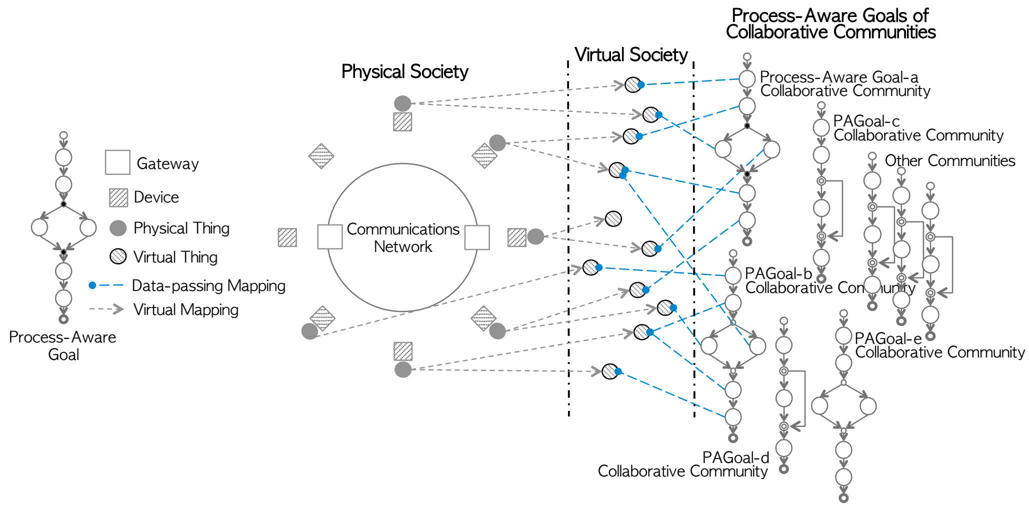

Fig. 1. A Conceptual Architecture of the Process-Aware IoT Community Computing Environment

autonomously) to accomplish it's goal[9]. The community is broken up and rejoin its members into the corresponding society after completing the goal. In this section, we simply introduce how to abstract the goal of the process-aware collaboration community to be modeled, deployed, and enacted over a process-aware IoT community computing environment.

Fig. 1 illustrates a conceptual architecture for the process-aware IoT community computing environment[10] that is arranged by physical IoT society, virtual IoT society, and a group of process-aware communities that can be statically, dynamically or autonomously formed out of smart-objects in the virtual IoT society. As shown in the conceptual architecture, the virtual IoT society spawns a series of collaborative communities, and the role of each community is to perform its own stepwise-activities described by a process-aware goal. The previous research of the authors proposed the process-driven IoT community computing model [1] as a formal description methodology for abstracting the concept[3] of process-aware goals in the IoT community computing environment. As the next step of the research, we concretize the concept and the model [1] *via* a process-aware goal description language with its XML-based schema.

III. XML Schema of the Process-Aware Goal Description Language

Based upon the process-aware IoT community computing model, we devise an XML-based description language designated for abstracting process-aware goals of the corresponding Internet of Things communities. The major constructs of the abstract language consist of activities, sourcing and sinking data repositories, and community-members. The activity construct is concretized by two types of roles: atomic role type and compound role type.

[3]Note that the **process-aware goal** is defined by a predefined or intended set of tasks or roles, called activities, and their temporal ordering of executions. A process-aware IoT-community computing system helps to organize, control, and execute process-aware IoT-communities by defining their process-aware goals that are represented by the process-aware IoT-community computing model proposed in [1].

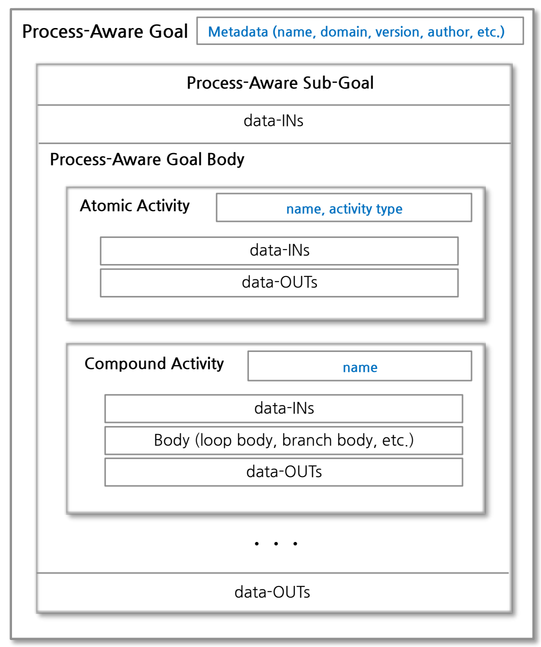

Fig. 2. The XML Schema Skeleton of the Process-Aware Goal Description Language

Fig. 2 shows the XML-based schema skeleton that is made up of four partitions with the primitive tag types—Metadata, data-INs, data-OUTs, and BODY—to build the textual representation of a process-aware goal. Assume that the accomplishment of a process-aware goal implies to perform all of the associated roles of the corresponding IoT-based collaborative community. In particular, the subGoal-BODY portion of a process-aware goal description language is composed of a bundle of procedural activities, each of which abstracts either atomic role or compound role. The detailed schema of the atomic roles type and the compound roles type are described in the following subsections. In terms of the notational XML syntax[8], the following are used to simplify the descriptive representations of the process-aware goals:

- Elements and attributes of XML tags may have one of the wildcard characters as follows: ? (0 or 1), ⋆ (0 or *more*), + (1 or *more*), # (*exclusive-existence*)
- Elements ending with "…" (e.g. <*element* … /> or <*element* … >) indicate that elements or attributes irrelevant to the context are being omitted.

A. The Activity Construct

The process-aware goal description language is used for the user to compose a process-aware goal by defining an abstract model as well as a concrete model. The abstract model is defined by a procedural combination of the activity constructs, while the concrete model is defined by associating either an atomic role or a compound role with each of the corresponding activity constructs. Eventually, those defined process-aware goals are deployed and enacted on the Internet of Things community computing environment.

```
<activity name="Name" type="Type" from="α1" to="α2">
  <data-INs>
        <data-IN name="Name" type="Type">
             <value> Constants </value>?
        </data-IN>⋆
  </data-INs>
  <atomic-ROLE name="Name" type="Type"/>#
  <compound-ROLE name="Name" type="Type"/>#
  <data-OUTs>
        <data-OUT name="Name" type="Type"/>⋆
  </data-OUTs>
</activity>
```

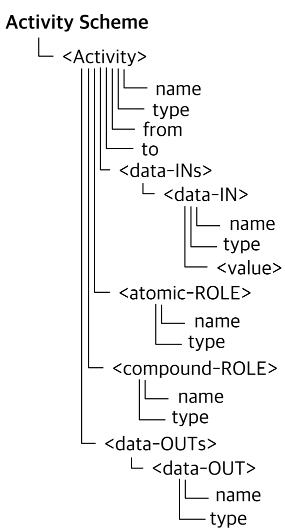

Fig. 3. The XML Scheme of the Activity Construct

Fig. 3 shows a graphical structure of the XML-based activity construct and its XML scheme with tag elements, such as data-INs, data-OUTs, atomic-ROLE, compound-ROLE, and attributes, such as name, type, from, to. A corresponding activity is exclusively concretized by associating with either an atomic role or a compound role. This association rule is represented by the tag elements of ROLE with the *exclusive-existence* wildcard character, #.

B. The Atomic Role Type

In the process-aware goal description language, the atomic role type is built by three tag elements: Metadata, data-INs, and data-OUTs. The metadata has a name property and a type property. The name property is an unique identifier of a corresponding atomic role; the type property characterizes its corresponding atomic role as a concrete service provided a specific task chosen from a group of tasks. Each task in the group is a concrete smart-object having a same functionality with probably different performances (behaviors, QoS characteristics, costs, etc.), and being implemented and deployed in the virtual society of the Internet of Things community computing environment. Assume that the affiliative information between atomic roles and concrete smart-objects is managed by the worklist registry component of a process-aware goal IoT community enactment system. Fig. 4 illustrates the XML scheme of the atomic role type with its XML language Skeleton.

```
<atomic-ROLE name="Name" type="Type">
 <data-INs>
   <data-IN name"Name" type="Type" source="Source"? >
     <value> Constants </value>?
   </data-IN>⋆
 </data-INs>
 <data-OUTs>
   <data-OUT name="Name" type="Type" saveto="Loc"? />⋆
 </data-OUTs>
</atomic-ROLE>
```

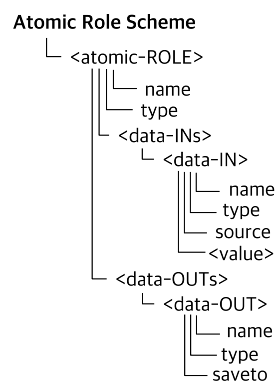

Fig. 4. The XML Scheme of the Atomic Role Type

C. The Compound Role Type

The process-aware goal description language is able to provide a rich set of compound role types. That is, the compound role type supports making a variety of collaborative formations in a group of roles, which is sub-classified into mesh-type, loop-type, and alternative-type formations. The mesh-type collaborative formation is represented by DAG (Directed Acyclic Graph) compound role; the loop-type collaborative formation is defined by FOR and WHILE compound roles; and the alternative collaborative formation is formatted by IF and ALT (Alternative) compound roles. In this section, we design the detailed XML schema and formats of those atomic role and compound role types after defining the XML scheme of the activity construct. In particular, we introduce only the DAG compound role type due to the page limitation. Fig. 5 illustrates the XML scheme of the DAG compound role type with its XML language Skeleton. A DAG compound role type is a commonly used type to express control flow dependencies among the affiliated atomic roles in a corresponding compound role. The possible formation of the control flow dependencies is classified into sequential and parallel dependencies inside of a DAG compound role.

```
<dag-ROLE name="Name" type="Type">
 <data-INs>
   <data-IN name"Name" type="Type" source="Source"? >
     <value> Constants </value>?
   </data-IN>*
 </data-INs>
 <atomic-ROLEs>
   <atomic-ROLE name"Name" type="Type" from="Role" >+
 </atomic-ROLEs>
 <data-OUTs>
   <data-OUT name="Name" type="Type" saveto="Loc"? />*
 </data-OUTs>
</dag-ROLE>
```

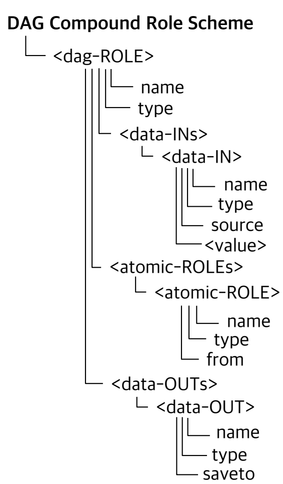

Fig. 5. The XML Scheme of the DAG Compound Role Type

IV. Related Works

So far, there exist several pervasive (or ubiquitous) community computing models[5][11] such as the context-aware community collaboration model[5], the society collaboration model[4][11], and the member collaboration model[6][11] for building an IoT-based pervasive community computing environment[1][10][12]. The context-aware community collaboration model[5] supports a community goal, which can be described by the goal description language proposed in this paper, through a series of situations from the initiating situation to the terminating situation in the corresponding community. Each of the member-objects fulfills its assigned role in a specific situation in the community. It is assumed that the defined community goal is accomplished if all of the member-objects achieve their assigned goals. Additionally, context-aware community collaboration models as the process-aware Internet of Things[10] can be classified into the three levels[11] of intellectualized community,*i.e.*, the simple collaboration model, the dynamic collaboration model, and the autonomous collaboration model, according to the degree of intellectualization. These models can be represented by the process-aware goal description language in this paper. The process-aware goal description language uses the society collaboration model[11] to define a group of activities, which is executable in a pervasive (or ubiquitous) intellectual mobile-space that are built upon the process-aware Internet of Things architecture and system[10].

V. Conclusion

In this paper, we have proposed an XML-based description language, which is so-called "process-aware goal description language," to specify process-aware goals of the Internet of Things communities. A process-aware goal is abstracted by a group of activities and their procedural and temporal combinations. Each activity is reified by either an atomic role or a compound role. Therefore, we devised a set of XML-based schema structures for the activity construct and its concrete components: atomic role type and compound role type. In particular, we described the detailed specification of the DAG (Directed Acyclic Graph) compound role type only in this paper. As future works, we have plans to extend the XML schema so as to express all the remaining compound role types, and implement a process-aware goal modeling system supporting the process-aware goal description language proposed in this paper.

References

[1] H. Ahn and K. P. Kim, "A process-driven iot-community computing model," *ICIC Express Letters*, vol. 8, no. 12, pp. 483–488, 2013.

[2] "Itu internet reports 2005: The internet of things," Executive Summary, International Telecommunication Union, 2005.

[3] Y. Jung and M. Kim, "Situation-aware community computing model for developing dynamic ubiquitous computing systems," *Journal of Universal Computer Science*, vol. 16, no. 15, pp. 2139–2174, 2010.

[4] e. a. Minkyo In, "Web of things (wot) standardization status," *TTA Journal*, vol. 138, pp. 79–84, 2011.

[5] e. a. Sangkeun You, "Smart mobile services - m2m technology and its standardization status," *Telecommunications Trends Analysis*, vol. 26, no. 2, pp. 50–60, 2011.

[6] K. Kim and C. A. Ellis, *Section II / Chapter VII. An ICN-based Workflow Model and Its Advances, Handbook of Research on BP Modeling*. Hershey, Pennsylvania, USA: IGI Global, ISR, 2009.

[7] C. A. Ellis, J. Wainer, A. Rembert, and K. Kim, "Investigations on stochastic information control nets," *Information Sciences*, vol. 194, pp. 120–137, 2012.

[8] J. Qin and T. Fahringer, *SCIENTIFIC WORKFLOWS, Programming, Optimization, and Synthesis with ASKALON and AWDL*. Springer, 2012.

[9] M. Skerlavaj, V. Dimovski, and K. C. Desouza, "Patterns and structures of intra-organizational learning networks within a knowledgeintensive organization," *Journal of Information Technology*, vol. 25, no. 2, pp. 189–204, Jan. 2010.

[10] M. Kim, H. Ahn, and K. P. Kim, “Process-aware internet of things: A conceptual extension of the internet of things framework and architecture,” *KSII Transactions on Internet and Information Systems*, vol. 10, no. 8, pp. 4008–4022, Aug. 2016.
[11] W. Cho, *u-SERVICE DESIGN: Ubiquitous Computing Experts Series*. Jinhan MB Publishing Co., 2009.
[12] D. Xu, W. H. Li, and S. Li, “Internet of things in industries: a survey,” *IEEE Transactions on Industrial Informatics*, vol. 10, no. 84, pp. 2233–2243, Jan. 2014.

Hyunah Kim Dr. Kim is an adjunctive professor and a faculty member of the collaboration technology research laboratory in the department of computer science at Kyonggi University, South Korea. She received her B.S. degree in computer science from Korea Nazarene University in 2001. Also, she received her M.S. and Ph.D. degrees in computer science from Kyonggi University in 2003 and 2009, respectively. She has been on the operational committees of several domestic and international conferences including KSII, AP-IST, ICONI, and ICACT. Her research interests include workflow systems, SCORM-based e-Learning process models, BPM, BPI, ACM, workflow-supported social networks discovery and analysis, and process-aware Internet of Things.

Kwanghoon Pio Kim Dr. Kim is a full professor of computer science department and the founder and supervisor of the collaboration technology research laboratory at Kyonggi University, South Korea. He received B.S. degree in computer science from Kyonggi University in 1984. And he received M.S. degree in computer science from Chungang University in 1986. He also received his M.S. and Ph.D. degrees from the computer science department at University of Colorado Boulder, in 1994 and 1998, respectively. He had worked as researcher and developer at Aztek Engineering, American Educational Products Inc., and IBM in USA, as well as at Electronics and Telecommunications Research Institute (ETRI) in South Korea. In present, he is a vice-chair of the BPM Korea Forum. He has been in charge of a country-chair (Korea) and ERC vice-chair of the Workflow Management Coalition. He has also been on the editorial board of the journal of KSII, and the committee member of the several conferences and workshops. His research interests include groupware, workflow systems, BPM, adaptive case management (ACM), CSCW, collaboration theory, Grid/P2P/Cloud distributed workflow systems, process warehousing and mining, workflow-supported social networks discovery and analysis, process-aware information systems, data intensive workflows, and process-aware Internet of Things.

Virtual Antenna Mapping MIMO Techniques in a Massive MIMO Test-bed for Backward Compatible LTE Mobile Systems

Seok Ho Won, Saeyoung Cho, Jaewook Shin
Mobile Communication Department,
Electronics and Telecommunications Research Institute, Daejon, Korea
shwon@etri.re.kr, csy1009@etri.re.kr, jwshin@etri.re.kr

***Abstract*—This paper proposes a virtual antenna mapping method for backward compatible massive or large-scale antenna multiple input multiple output (MIMO) base stations that provide communication services for legacy user equipment (UE) that can recognize only two or four base station antennas. The proposed method adopts and improves the omnidirectional beamforming that has been pioneered in previous works with proposing new method of determining antenna array coefficients through shifting the discrete Fourier transform (DFT) basis vectors for Zadoff-Chu (ZC) sequences. In the proposed method, the number of the parameters to be optimized is only two although the number of transmit antennas is hundreds or more (e.g., 500 antennas was proved in the paper as an example). Moreover, with the independent properties of the shifted versions of ZC sequences, this paper proves the fact that the coefficient vectors consisting virtual transmit antennas are independent when the channel gains work as the coefficients of them. This characteristic gives diversity with the pre-codes because two pre-code vectors must independent which means their linear combination with the non-zero channel gains or coefficients cannot be zero. The computer simulation results provide four important findings; the most important is that the actual number of virtually mapped physical antennas is inversely proportional to the transmit power per antenna.**

***keyword*—massive MIMO, virtual antenna techniques, omnidirectional beamforming, transmit diversity, precoding techniques**

I. INTRODUCTION

Along with small cell technology, massive multiple input multiple output (MIMO) is a promising technology for increasing the capacity to fulfil the potential traffic increases in next-generation mobile communication systems [1]. While small cell technology can increase capacity through reducing the cell radius, massive MIMO adopts a large scale for the transmit antennas. In small cell technology, in order to reduce the cell radius, the macro base station extends its antennas with some radio parts called 'remote radio heads' (RRHs) through connecting them with optical fibers, which results in high installation costs [1]. In contrast, by collocating many antennas to save the connecting costs massive MIMO technology has a relatively cheaper installation cost than the small cell technology [1]. Furthermore, massive MIMO has many radio frequency (RF) chains and antennas; thus, the transmission power per antenna decreases given that total transmission power is constant, which also results in decreasing RF part costs. Moreover, theoretically, massive MIMO technology can eliminate fast fading while increasing throughput and terminal numbers independent of the cell size [1-3]. Therefore, we designed massive MIMO test-bed as the pilot for next-generation mobile systems and future LTE-A system [4].

For a massive MIMO base station, dozens of or even hundreds of transmitting antennas are essential to give the effects described above. However, currently the LTE-A specification (e.g., Release-10 or later versions) allows eight transmit antennas and is expected to have more transmit antennas in the future [5, 6]. Therefore, just for analogy purpose, we first restrict the number of transmit antennas to eight in the paper although the massive-MIMO test-bed will have much more transmit antennas. However, with the simple example it is shown the possibility of extending them to hundreds by using the proposed method (e.g., 500 antennas in Figure 3b in this paper).

As for the backward compatibility, LTE-A eNode-B (i.e., base station) that has eight (or more) transmit antennas should provide service to legacy LTE (e.g., Release-8, 9) UEs that can recognize only two or four transmission antennas of eNode-B without notifying any information through additional control channels or signaling. Therefore, this paper introduces virtual antenna technique that can improve UE performance without increasing complexity of UE or eNode-B.

The proposed virtual antenna technique or backward compatible MIMO technique that converts eight physical transmit antenna to two or four logical antennas uses pre-codes that enable UE to use wireless channel's degrees of freedom and diversity efficiently by having robustness for high spatial correlations. In order to give diversity with the pre-codes, two pre-code vectors must independent which means their linear

Manuscript received November 9, 2016. This work was supported by Institute for Information & communications Technology Promotion (IITP) grant funded by the Korea government (MSIP) (No. R0101-15-244, Development of 5G Mobile Communication Technologies for Hyper-connected smart services) and a follow-up of the invited journal to the accepted & presented the out-standing paper of the 17th International Conference on Advance Communication Technology (ICACT2015).

Seok Ho Won is with the Department of Wireless Transmission Research, ETRI (Electronics and Telecommunications Research Institute), Korea (Corresponding author, phone: +82-42-860-5449 e-mail: shwon@etri.re.kr.)

S. Cho and J. Shin are with Mobile Giga Transmission Research, ETRI, Korea (e-mail: csy1009@etri.re.kr; jwshin@etri.re.kr)

combination with the non-zero channel gains or coefficients cannot be zero. The generation method for pre-coding matrix is similar but not same with cyclic delay diversity (CDD) that current LTE specification defines. The validation of the performance is proved by computer simulation because in the design stage, computer simulations can also be useful for good designing while test-beds are used in lab tests as a replacement for field tests.

In the following chapter, we introduce proposed virtual antenna mapping as the backward compatible MIMO techniques in massive MIMO test-bed with key technique of omnidirectional beamforming (OB), and we discuss about the transmitter and receiver structure for legacy user equipment (UE). Next, we evaluate the proposed method with some assumption for simple analysis. After evaluation, we conclude the paper with some important findings.

II. Proposed Virtual Antenna Mapping

The proposed virtual antenna mapping that converts eight physical transmit antenna to two or four logical antennas is based on the OB as shown in Figure 1. With a OB beam, we can have two or four orthogonal beams by phase shifting of the beam precoding vector of the OB beam as we will show later.

A. Omnidirectional Beamforming (OB)

The simplest way to make OB beam is sending transmit signal through only one antenna but this make the all transmit signal power converged into only one antenna and all power signals flow the radio frequency (RF) circuits of that antenna path only. As a result, high cost RF circuits like high power amplifier (HPA) must be needed [7]. Therefore, we can have following two requirements (RQs) for OB:

- RQ1. All radiating power for each transmit antenna in the MIMO BS must be equal or nearly equal.
- RQ 2. The gains of beam pattern have the least variations within the angle range of the service sector (e.g., 120 degree for 3 sector cell).

To find OB with above RQs, pioneering technique called random beamforming (RBF) has been used [7-9]. We make RBF fancier technique by approaching the problem for satisfying above RQs with more systematic way of using the duality property of the digital Fourier transform (DFT) instead of using randomness which is described in next few paragraphs.

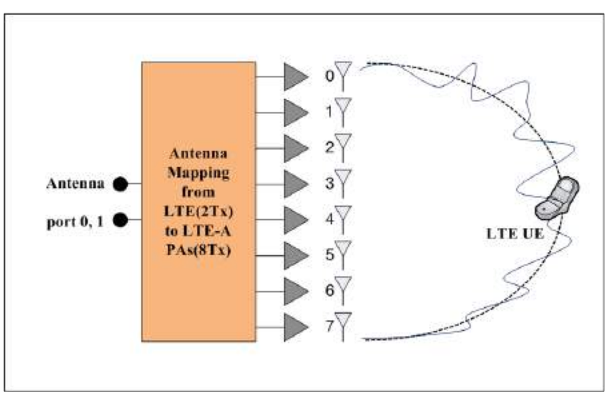

Fig. 1. Virtual antenna mapping concept for backward compatible MIMO techniques

As the initial model, planer array antennas are commonly used and practical model can be develop based on this simple starting model. Therefore, for a simple analysis this paper assumes the system of using a uniform linear array (ULA) antenna and the beamforming array vector is given as follows [10]:

$$\overline{a}\left(\theta\right)=\left[1,e^{-j\frac{2\pi}{\lambda}d\sin(\theta)}\ ,\ \ldots\ ,\ e^{-j\frac{2\pi}{\lambda}(M-1)d\sin(\theta)}\ \right]^{T} \quad (1)$$

where λ is the RF wave length, d is the distance between two adjacent antenna elements, θ is the angle variable representing the direction of the beam pattern generated by the beam steering vector. Note that the analysis in reference [11] uses ϕ the angle of incidence of the line-of-sight onto the transmit antenna array instead of using θ (i.e., $\theta{=}\frac{\pi}{2}{-}\phi$) and so uses directional cosine (i.e., $\Omega{:=}\cos(\phi)$) constructing the unit spatial signature for the angular domain analysis [11].

Suppose that $\overline{w}$ is the weight coefficient vector with complex number entries $\{w\left(m\right),\quad m=0,1,\ \ldots\ ,M-1\}$ for the antenna elements where M is the total number of base station antennas. Then the resulting beam pattern transmitted by the total base station transmit antennas can be expressed as follows [10]:

$$G\left(\theta\right)=\ \overline{w}^{H}\cdot\overline{a}(\theta)\ =\ \sum_{m=0}^{M-1}w^{*}(m)\cdot e^{-j\frac{2\pi}{\lambda}mdsin(\theta)}. \quad (2)$$

Let's define a function $\mathit{\Omega}(\theta)\ :=\frac{2\pi}{\lambda}dsin\left(\theta\right)$ and use this as the substitution variable. Note that reference [11] defines directional cosine (e.g., $\Omega{:=}\cos(\phi)$) instead of $\mathit{\Omega}\left(\theta\right)$ defined in this paper. Through the substitution, the beam pattern can be expressed as follows:

$$\begin{aligned}G\left(\theta\right)=\quad & W\left(\mathit{\Omega}\left(\theta\right)\right)=\sum_{m=0}^{N-1}w(m)\cdot e^{-j\mathit{\Omega}(\theta)m}\\ or\quad & W\left(\mathit{\Omega}\right)=\sum_{m=0}^{N-1}w(m)\cdot e^{-j\mathit{\Omega}m}\ .\end{aligned} \quad (3)$$

This equation is a discrete-time Fourier transformation (DTFT) that transforms the discrete-time signal $w(m)$ with a finite duration into a continuous and periodic frequency signal $W(\mathit{\Omega})$. Therefore, using the inverse DTFT (IDTFT) for (3), we can obtain the sequence elements as follows:

$$w\left(m\right)=\ \frac{1}{2\pi}\int_{2\pi}W\left(\mathit{\Omega}\right)\cdot e^{j\mathit{\Omega}m}\ d\mathit{\Omega}. \quad (4)$$

As a result, our problem refers to finding the sequence $\{w\left(m\right),\quad m=0,1,\ldots,M-1\}$ through simply performing the IDTFT of the continuous beam pattern $W\left(\mathit{\Omega}\right)$ that was originally from $G(\theta)$ whose variance is minimal. Therefore, the sequence must be satisfied regardless of the domains that it is transformed to using (3) and (4) (i.e. DTFT and IDTFT), and the amplitude or power of each element of the sequence must be constant. The typical sequence with those characteristics is Zadoff-Chu (ZC) sequence and it is expressed as follows [12]:

$$s(m) = e^{-j\pi\mu m\ (m+\langle M\rangle_2)/M}, \tag{5}$$

where μ is an integer less than and relative coprime to M and the notation $\langle x\rangle_y$ denotes the remainder of x modulo y. Through inserting the circular shift parameter k into (5), we can obtain following equation:

$$\begin{aligned}\alpha(m) &:= s(m+k) \\ &= e^{(-j\pi\mu(\langle m+k\rangle_M)\ (\langle m+k+\langle M\rangle_2\rangle_M)/M}.\end{aligned} \tag{6}$$

With (6) and given the total number of base station transmit antenna elements M, the goal becomes narrowing this to locate only two parameters of μ and k that can generate the unique circular-shifted ZC sequence with a large number of elements. Our goal is to make OB in angular domain which gets discrete coefficients for each antenna element through IDFT: so we can make resulting beam generated by the antennas in the original angular domain which will be the target constant amplitude beam again. Therefore, by considering beam steering vectors as the DFT operators, we choose the weighting sequence whose amplitude remains constant before and after DFT.

B. Parameter Optimization Procedure

In order to optimize parameter values for the antenna coefficient sequences, we first look at the relationships between antenna elements and beam patterns. Figure 2 shows the relationship of the sequence with the antenna weights $\{w(m),\ m = 0,\ 1,\ ..,\ M\}$, approximated beam pattern $W(\Omega)$, and exact beam pattern $G(\theta)$ (see upper parts of the figure). The antenna weights $w(m)$ are transformed to approximated beam pattern $W(\Omega)$ by DTFT, and turn further into exact beam pattern $G(\theta)$ by the variable substitution process (see the upper part of the figure). In the process of the variable substitution and given the array length L for the array antennas, the sine domain or directional cosine domain (i.e., Ω domain) has uniform resolution ($\frac{1}{2L}$) but the angular domain (i.e., ϕ domain) has non-uniform resolution [11]. With these relationships analysed in this paper, interesting readers can solve the exercise 7.8 in [11].

Figure 2 also shows the relationship between discrete Fourier transform (DFT) and DTFT to identify the sampling errors occurred in the process of converting signals between digital and continuous domains (see the lower box in the middle part of the figure). The sampling errors also give severe effects to increasing the variance of beam pattern and these errors can be decreased as the M increases, which are favorable to massive MIMO systems. With these relations, the idea of the proposed method come from the fact that Fourier transform or its inverse transform of the ZC sequences can change the total average sequence amplitude and phases but can not change the amplitudes or powers of the sequence elements independently by the properties of the sequences as described in the bottom of the figure. For parameter optimizing procedures, up to date the most pioneered method has turned out to be the method of Yang, et. al.'s [7] which we follows in the point of variance minimizing target. Assume that for entire section $\{\theta_1 \le \theta \le \theta_2 \mid \theta_1 = 0,\ \theta_2 = 2\pi\}$ and $\mathrm{d} = \lambda/2$ then the expected value of $|G(\theta)|^2$ is given as M (i.e., $\mathrm{E}\left[|\mathrm{G}(\theta)|^2\right] = \mathrm{M}$) [7]. Therefore, by using (2) and (4), the square variance can be calculated as follows (the detailed solving procedures are given in [7]).

$$\begin{aligned}\sigma^4 &= \frac{1}{2\pi}\int_0^{2\pi}\left(|G(\theta)|^2 - M\right)^2 d\theta \\ &= \frac{1}{2\pi}\int_0^{2\pi}\left(\left|\sum_{m=0}^{M-1} e^{-j\psi_m}\cdot e^{-j\pi m\ sin(\theta)}\right|^2 - M\right)^2 d\theta \\ &= \sum_{j=1}^{M-1}\sum_{m=1}^{M-j}\sum_{n=1}^{M-j} cos(\psi_{m+j} - \psi_m - (\psi_{n+j} - \psi_n)).\end{aligned} \tag{7}$$

Yang, et. al. obtained the optimum patterns by taking the partial derivatives with respect to ψ_m to reach the minimum value of σ^4. However, it is usually too complex to find the solution especially when the number of variables to find is several hundred with the common massive MIMO system nature.

Instead of using the partial derivative method, this paper uses relatively simple algorithm called the simplex search

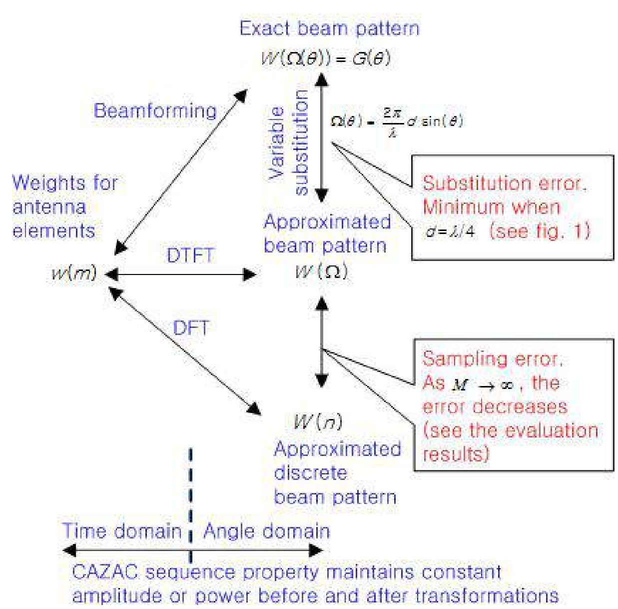

Fig. 2. The relationships for the antenna weights $w(m)$, approximated beam pattern $W(\Omega)$, and exact beam pattern $G(\theta)$. Important error sources of the sequences are also shown in two boxes located in right side.

method of Lagarias et. al. [13] which is a direct search method that does not use numerical or analytic gradients with expanding the method to n-dimensional space. While Yang's method tried to optimize M variables for the antenna elements, the proposed method tries to optimize only two variables of the parameters μ and k in (6) to make the sequence uniquely determined. Therefore, by substituting $\alpha(m)$ in (6) to $w(m)$ for (2) and (3), we can get following equation:

$$\sigma^4 = \sum_{j=1}^{M-1}\sum_{m=1}^{M-j}\sum_{n=1}^{M-j} cos(\Psi_{m+j+k}-\Psi_{m+k}-(\Psi_{n+j+k}-\Psi_{n+k})) \tag{8}$$

where $\Psi_x = -\pi\mu(\langle x\rangle_M)(\langle\langle x+\langle M\rangle_2\rangle\rangle_M)/M$.

While the beam pattern square variances σ^4 in (7) and (8) look alike, the functions Ψ_x and ψ_m are defined differently. More precisely, the phase function of the sequence in (8) is more general form and that in (7) is specific form.

Figure 3a shows the polar plot for the found optimum antenna weights for 32 antenna elements $\{w^*(m), m{=}\ 0,1,\ldots,\ 31\}$. These sequence is generated by the circular shifted Zadoff-Chu sequence rule with the optimized parameters of $\{\mu^*{=}\ 1, k^*{=}\ 1\}$ which are founded by using the simplex search method with the initial value of $\{\mu_o{=}\ 1, k_o{=}\ 1\}$ also for the proposed method. The computed values for them are $\{\mu^*{=}\ 1.0157, k^*{=}\ 0.7366\}$ with the proposed method (see Figure 4). However μ must be the relative coprime to the number 32 and k must be integer: so we choose them for the closest numbers that satisfy these conditions for the sequence. Figure 3b shows the same case with the Figure 3a except for the number of transmit antenna elements of 500.

The parameters for this sequence do not need to be found but predicted by the fact shown in the Figure 4 which shows the change trends for two optimized parameters $\{\mu^*,\ k^*\}$ for the circular shifted Zadoff-Chu sequence as the number of transmit antenna increases. In the figure, they are converged into special value but we choose them for the closest numbers that satisfy these conditions for the sequence (i.e., relative coprime and integer).

To compare practical usefulness for the conventional method and proposed method in this paper, suppose the massive MIMO system that has 100 transmission antenna elements. Then, the number of variables to find in the proposed method decreases 50 times (i.e., 100:2) in these example procedures. Moreover, we found in the proposed method the optimum values of the two parameters of μ and k changed with nearly negligible values as shown in above. Therefore, the proposed method can give good approximation information to the future analysis for the massive MIMO system with theoretically infinitive number of transmit antenna elements for (i.e., $M \to \infty$).

C. Virtual Antenna Mapping

Let DFT matrix be denoted by $\underline{\mathrm{v}} := [v_1, v_2, \cdots, v_N]$ and $\{v_i, \quad i = 1, 2, \ldots, N\}$ are the column vector set for the DFT matrix. Further, suppose the first weighting sequence can be expressed as follows.

$$\overline{w}_0^{(1)} = \sum_{\mathrm{i}=2}^{\mathrm{N}-3} \alpha_{\mathrm{i}} \mathrm{v}_{\mathrm{i}} \tag{9}$$

where $\forall$i, $|\alpha_{\mathrm{i}}| = 1$ for i-th complex scalar sequence to satisfy RQ1. In (9), we truncate the sequence or use only i=2,...,N-3 instead of using all N elements of the sequence which means just only partial sequence elements can be used for the weights. Next, to fulfil RQ2 we can get the first OB weight $\overline{w}_0^{(1)}$ by choosing and truncating the weighting sequence which satisfies (10) as follows.

$$\alpha_{\mathrm{i}}^* = \underset{\{\alpha_{\mathrm{i}},\ \mathrm{i=m,\ldots,n}\}}{\mathrm{argmin}} \sqrt{\frac{1}{\theta_2-\theta_1}\int_{\theta_1}^{\theta_2} \left(|G(\theta)|^2 - E[|G(\theta)|^2]\right)^2 d\theta} \tag{10}$$

where G(θ) is given by (2) and $E[\cdot]$ denotes the expect value operator.

With an OB beam, eNode-B can map one virtual antenna port to multiple physical antennas (e.g., 8 transmit power

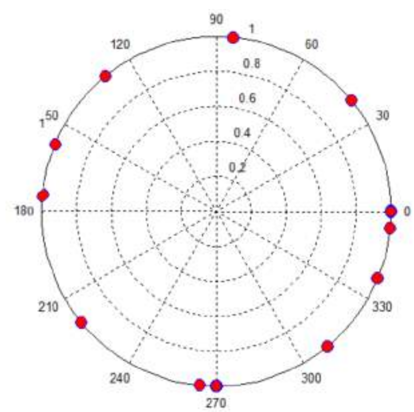

(a)

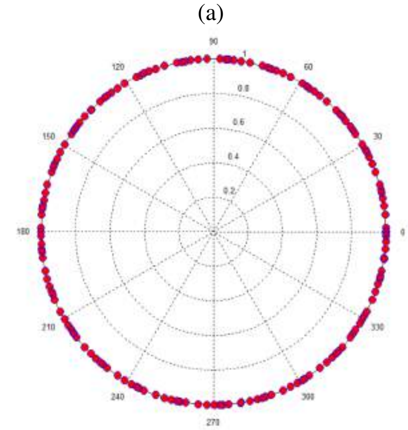

(b)

Fig. 3. Polar plot for the found optimum antenna weights for { (a) 32, (b) 500 } antenna elements $\{w^*(m),$ $m{=}\ 0,1,\ldots,\ 31$ or $499\}$ by the proposed method. Some values are overlapped.

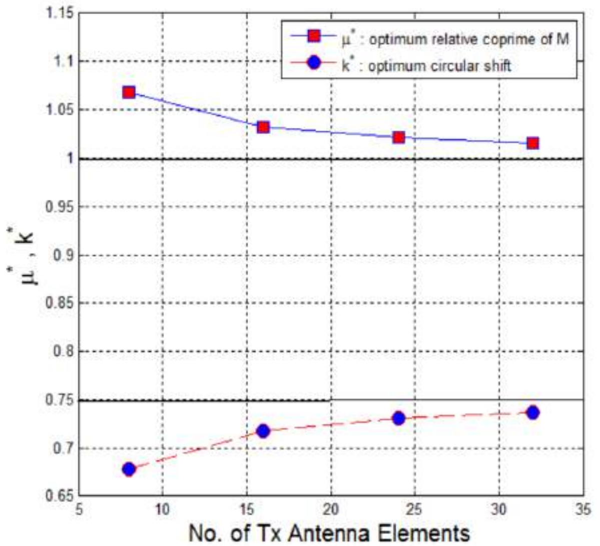

Fig. 4. Optimum circular shifted Zadoff-Chu sequence parameter value change as the number of transmit antenna elements increase for the proposed method

amp and antennas). To get one more virtual antenna port for diversity transmission, we need to get the second OB beam and this is given by $\overline{w}_0^{(2)}$ as the circular shifted version of $\overline{w}_0^{(1)}$ as follows.

$$\overline{\mathrm{w}}_0^{(2)} = [\ldots,\ \mathrm{w}_{\mathrm{N}-3}^{(1)}, \mathrm{w}_{\mathrm{N}-2}^{(1)}, \mathrm{w}_{\mathrm{N}-1}^{(1)},\ \mathrm{w}_0^{(1)},\ \mathrm{w}_1^{(1)},\ \ldots] \tag{11}$$

With the same manner, we can get third and fourth OB beams for four virtual antenna ports. However, we consider two OB beams for two virtual antenna ports and more than two OB beam case is left for future study.

In order to give diversity between two virtual transmit antennas, the coeficient vectors $\overline{w}_0^{(1)}$ and $\overline{w}_0^{(2)}$ must be independent when the channel gains work as the coefficients of them. Therefore, theorem 1 must be justified.

Theorem 1. *Two vectors $\overline{\mathrm{w}}_0^{(1)}$ and $\overline{\mathrm{w}}_0^{(2)}$ generated by she shifted versions of ZC sequence are independent.*

Proof. Suppose that $\overline{\mathrm{w}}_0^{(1)}$ and $\overline{\mathrm{w}}_0^{(2)}$ are dependent. Then there exits non-zero coefficients $c_1,\ c_2$ such that $\mathrm{c}_1\ \overline{\mathrm{w}}_0^{(1)} + c_2\overline{\mathrm{w}}_0^{(2)} = 0$. However, $\overline{\mathrm{w}}_0^{(1)}$ and $\overline{\mathrm{w}}_0^{(2)}$ are ZC sequences and with the auto-correlation property they are orthogonal each other and cannot be represented by linear combination of the other vector. □

With the manner described above, we can get sequences for beams 0 and 1 for eight physical antennas with power amplifiers (PAs) and example sequence values are shown in Table I. With the two OB beams of equations (9) and (11), the MIMO BS can map the two antenna ports to these two beams respectively. As an application example of the method for the traffic signals of the legacy UEs, cell-specific reference signals (CRSs) for diversity transmission with two antenna ports can be denoted by CRS0 and CRS1 and they can be directly mapped to OB beam 0 and 1 respectively. With the same manner, the two physical broadcasting channel (PBCH) symbols for transmit diversity (e.g., Alamouti coded two symbols) can be mapped to OB beam 0 and 1 respectively.

TABLE I
GENERATED BEAM WEIGHTING SEQUENCES

Beam 0 (e.g., $\overline{\mathrm{w}}_0^{(1)}$)	**Beam 1 (e.g., $\overline{\mathrm{w}}_0^{(2)}$)**
0.10406 + j*(-0.24340395)	-0.10406 + j*(+0.243403)
0.21346 + j*(-0.16386)	0.21346 + j*(-0.163868)
0.33082 + j*(+0.15179)	-0.33082 + j*(-0.151797)
-0.16340 + j*(+0.38933)	-0.16340 + j*(+0.389337)
-0.01444 + j*(-0.31956)	0.01444 + j*(+0.319562)
-0.08058 + j*(+0.40658)	-0.08058 + j*(+0.406583)
0.40698 + j*(+0.03329)	-0.40698 + j*(-0.033293)
0.20309 + j*(-0.25417)	0.20309 + j*(-0.254177)

D. Base Station's Transmitter Structure for Legacy UEs

With the method described in previous chapter, we know how to get virtual antenna mapping. To find most efficient way to use the mapping for base station's transmitter, we now consider two virtual antenna ports for the transmitter with eight physical antennas with following mapping cases:

- Case 1. Each port maps to two physical antennas with turning off the rest of the antenna PAs
- Case 2. Each port maps to two identical OB beams
- Case 3. Each port maps to two orthogonal OB beams with open loop space time block code (STBC)
- Case 4. Each port maps to two orthogonal OB beams with closed loop feedback for codebook index

Case 1 violates RQ1. and Case 2 has no diversity gain for two identical beams mapped by two virtual antenna ports, which will be proved at the evaluation chapter. On the other hand, Case 3 has diversity gain for two orthogonal beams mapped by two virtual antenna ports and used for STBC encoding as shown in Figure 5. This fact will be also proved at the evaluation chapter. For Case 4 we consider the transmitter and receiver mechanism shown in Figure 6. For the Case 4, we used LTE codebook index as shown in Table II [5].

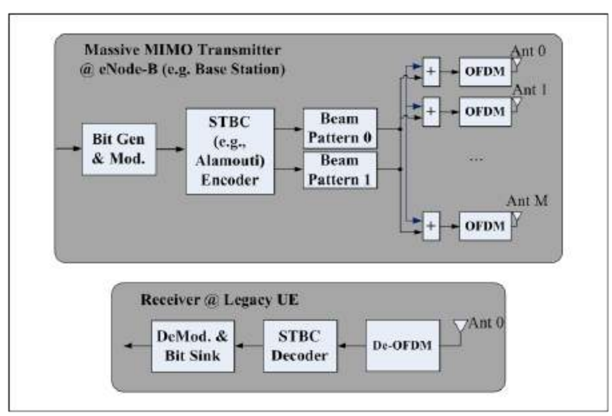

Fig. 5. Transmitter and receiver structure for Case 3

The codebook indices zero and one have zero valued element which means turning off the counterpart virtual antenna OB beam. The other codebook indices except those two show power distribute equally for the two beams which means equally combining of the two beams. The element's negative sign and imaginary component are intended to work for the signal phase change; so we can easily predict Case 3 and 4 will show the double (3 dB) performance difference which proved by the computer simulation results shown at the evaluation chapter.

TABLE II
CODEBOOK FOR CASE 4

Id	0	1	2	3	4	5
Vl	$\begin{bmatrix}1\\0\end{bmatrix}$	$\begin{bmatrix}0\\1\end{bmatrix}$	$\begin{bmatrix}s\\s\end{bmatrix}$	$\begin{bmatrix}s\\\bar{s}\end{bmatrix}$	$\begin{bmatrix}s\\js\end{bmatrix}$	$\begin{bmatrix}s\\j\bar{s}\end{bmatrix}$

$*s = \frac{1}{\sqrt{2}}, \bar{s} = -s$

III. Evaluation

Proposed virtual mapping method for backward compatible MIMO is evaluated by the computer simulations.

A. Computer Simulation Setup and Method

The computer simulation parameters are set as shown in Table III. Transmitters at eNode-B and UE receiver are set according to the Cases 1 - 4 described in above section.

TABLE III
SIMULATION PARAMETERS

Parameter	**Values**
Antenna configuration	8 elements, ULA, d $=\lambda/2$
Modulation	QPSK
Channel model	Random fading (not change for one frame duration and uncorrelated between antenna paths)
Packet length	4x130 bits/packet (260 symbols/packet or QPSK)
CSI feedback period (for Case4)	1 frame

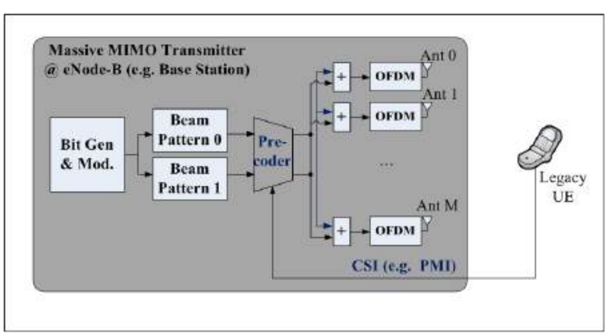

Fig. 6. Transmitter and receiver structure for Case 4.

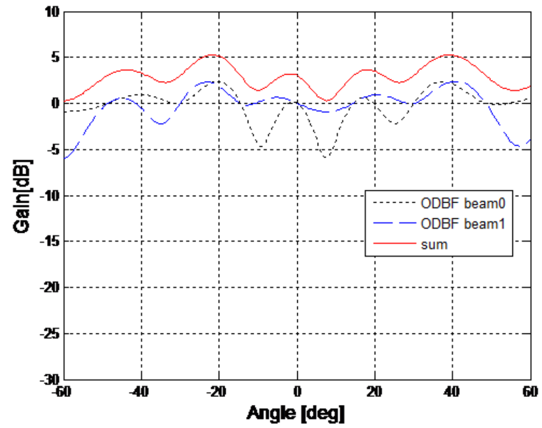

Fig. 7. Gains and their sum of the two OB beams

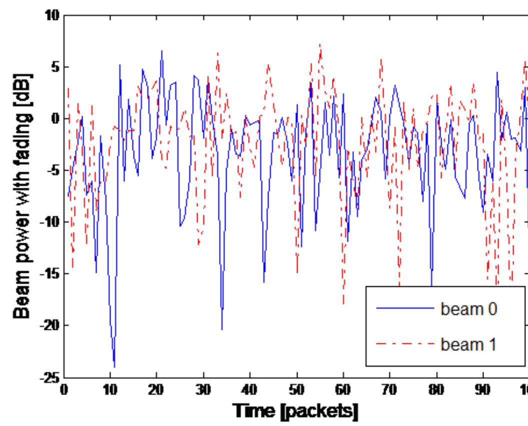

Fig. 8. Beam power variations with time for two orthogonal beams

B. Simulation Results and Discussion

Figure 7 shows the gains and their sum of the two draft OB beams obtained by the equations (9) and (11) that have example weighting sequences shown in Table 1. Approximately, each beam 0 and 1 fluctuates with 5 dB as the figure shows. However, we can get more flat OB beams by tuning the parameters of the equations but we leave this future study.

Figure 8 shows beam power variations with time for two orthogonal beams. In the figure, the power difference between the two beams shows distinctively and so gives diversity gain which can be seen in the Figure 9.

Figure 9 shows uncoded bit error rate (BER) performance versus transmit power per antenna for QPSK (a) and 16QAM (b). These figures as the simulation results give us following four findings:

i) Approximately, the uncoded BER results for the Case 3 and Case 4 are 6 dB (4 times) more than that of Case 1.
ii) Approximately, the uncoded BER results for the Case 4 are 3 dB (2 times) more than that of Case 3.
iii) The curve for Case 1 is steeper than that for Case 2.
iv) The uncoded BER performance results for QPSK and

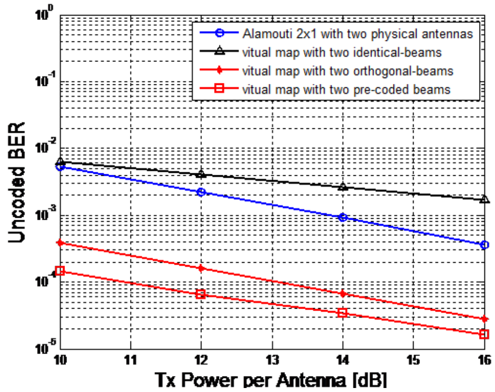

(a)

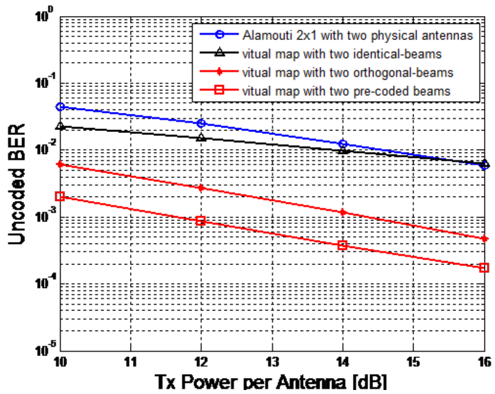

(b)

Fig. 9. Uncoded bit error rate performance versus transmit power per antennna: (a) QPSK, (b) 16QAM

16QAM show the same trend but the power difference shows 6 dB approximately.

The reason of i) is that with the same total powers of all transmitting physical antenna for each case the power per antenna is different. That is, Case 3 and Case 4 use eight transmit antennas while Case 1 uses two which result is four times (6 dB) power difference. The reason for ii) is that codebook index feedback of the Case 4 results in combining diversity gain and the phase control of the two beams. For example, the index (Id) 0 and 1 in Table 1 have the values (Vl) $[1,\ 0]^T$ and $[0,\ 1]^T$ respectively which mean full transmit power allocation for the good transmission antenna path while no power allocation for the bad. Therefore, the BER performance becomes as double as the open loop transmit diversity (Case 3). For the fact of iii), Case 2's two identical beams show no diversity gain as Case 1 of STBC encoding which result in steeper uncoded BER curve. From the iv), we can predict high order modulation (e.g., 64QAM) can work with the same trend and can be adopted in the proposed scheme.

IV. Conclusion

This paper proposed a virtual antenna mapping method for backward compatible massive MIMO base stations in order to provide communication services for legacy user equipment that can recognize only two or four antennas. The proposed method adopts the omnidirectional beamforming that satisfies the two research questions defined in this paper, and it provides a more systematic approach than previous pioneering works, as discussed in the introduction. The proposed method is to determine antenna array coefficients through shifting the discrete Fourier transform (DFT) basis vectors for Zadoff-Chu (ZC) sequences. With this method, this paper showed the possibility of extending the number of transmit antenna to hundreds (e.g., 500 antennas in Figure 3b in this paper) with only two parameters to be optimized. Moreover, with the independent properties of the shifted versions of ZC sequences, this paper proved the fact that the coefficient vectors consisting virtual transmit antennas are independent when the channel gains work as the coefficients of them. This characteristic enables the communication link having diversity with the two or more virtual transmit antennas. That is, in order to give diversity with the pre-codes, two pre-code vectors must independent which means their linear combination with the non-zero channel gains or coefficients cannot be zero. This paper also provides four types of transmitting structures at the base station in order to demonstrate the performance of the proposed virtual antenna mapping, and it derives four findings through a simple computer simulation (see Chapter III-B). Among these findings, the most important is that a four times (6 dB) higher uncoded BER performance was achieved when mapping eight physical antennas compared with that of mapping two physical antennas. Therefore, the actual number of mapped physical antennas is inversely proportional to the transmit power per antenna.

References

[1] A. Chockalingam and B. Rajan, *Large MIMO Systems*, Cambridge University Press, 2014.

[2] T. L. Marzetta, "Noncooperative cellular wireless with unlimited numbers of base station antennas," *IEEE Trans. Wireless Commun.*, vol. 9, pp. 3590-3600, Nov. 2010.

[3] F. Rusek, D. Persson, B. K. Lau, E. G. Larsson, T. L. Marzetta, O. Edfors, and F. Tufvesson, "Scaling up MIMO: Opportunities and challenges with very large arrays," *IEEE Signal Processing Mag.*, 2012.

[4] S. H. Won, S.C. Chae, S. Y. Cho, I. Kim, and S. C. Bang, "Massive MIMO test-bed design for next-generation long term evolution (LTE) mobile systems in the frequency division duplex (FDD) mode," Information and Communication Technology Convergence (ICTC), 2014 International Conference on, Busan, Korea, 2014.

[5] 3GPP, Evolved Universal Terrestrial Radio Access (E-UTRA); Physical Channels and Modulation (Release 11), TS 36.211 v11.2.0 (2013-02), http://www.3gpp.org/ftp/Specs/archive/36_series/36.211/36211-b20.zip

[6] 3GPP, "Study on Elevation Beamforming/Full-Dimension (FD) MIMO for LTE," technical document number RP-141644, 2014. http://www.3gpp.org/ftp/tsg_ran/TSG_RAN/TSGR_65/Docs/RP-141644.zip

[7] X. Yang, W. Jiang, and B. Vucetic, "A random beamforming technique for omnidirectional coverage in multiple-antenna systems," *IEEE Trans. Veh. Tech.*, vol. 62, pp. 1420-1425, Mar. 2013.

[8] J. Wei and X. Yang, "An enhanced random beamforming scheme for signal broadcasting in multi-antenna systems," Personal Indoor and Mobile Radio Communications (PIMRC) 2012.

[9] J. Chung, C. Hwang, K Kim, and Y. Kim, "A random beamforming technique in MIMO systems exploiting multiuser diversity," *Sel. Areas in Comm.*, vol.21, issue 5, pp. 848-855, June 2003.

[10] J. Litva and T. Lo, *Digital Beamforming in Wireless Communications*, Artech House, 1996.

[11] D. Tse and P. Viswanath, *Fundamentals of Wireless Communication*, Cambridge University Press, 2004.

[12] C. Chu, ”Polyphase codes with good periodic correlation properties,” *IEEE Trans. Inf. Theory*, vol. IT-8, pp. 531-532, 1972.
[13] J. Lagarias, J. Reeds, M. Wright, and P. Wright, ”Convergence properties of the Nelder–Mead simplex method in low dimensions,” *SIAM Journal on Optimization*, vol. 9.1, pp. 112-147, 1998.

Seok Ho Won received his B.S. degree in clinical pathology and electrical engineering from Kwangwoon University, Seoul, Rep. of Korea, in 1985 and 1990, respectively, and his Ph.D. degree in electrical engineering from Chungnam National University, Daejeon, Rep. of Korea, in 2002. Since 1985, he has been a clinical pathologist at Sin-Chon General Hospital, Gyeonggi-do, Rep. of Korea. Since 1990, he has been a principal engineer at ETRI, Daejeon, Rep. of Korea. He was a research faculty member at Virginia Tech, USA, in 2005. His research interests include information theory, error correction coding, MIMO, and beamforming with an emphasis on mobile communications.

Saeyoung Cho received the B.E. and M.E. degrees in department of Electronic and Information Engineering for Chonbuk National University, Jeonju, Chonbuk, Korea in 2008 and 2010, respectively. Since 2011, he has been with Electronics and Telecommunications Research Institude, Daejon, Korea, where he is the Research Staff of Wireless transmission research department. His research interests include digital communication and MIMO OFDM system.

Jaewook Shin received the M.S. degree from the Kyungpook National University, South Korea in 1994 and Ph.D. degree in computer science from the Chungnam National University, South Korea in 2005. He has been working for Electronics and Telecommunications Research Institute (ETRI) as a researcher since 1994. He was a visiting researcher at the University of California, Irvine in 2012. He is currently a director of radio transmission technology section in ETRI. His current research interests include 5G mobile telecommunication, D2D and M2M.

Experimental Validation of Multipoint Joint Processing of Range Measurements via Software-Defined Radio Testbed

Georgy Mashkov*, Eugene Borisov*, Grigorii Fokin*

* State University of Telecommunication, 22 Prospekt Bolshevikov, St. Petersburg, Russia

MashkovGM@sut.ru, kafedra@sut.ru, grihafokin@gmail.com

***Abstract*—In this paper we present an algorithm for multipoint positioning in multilateration (MLAT) radio navigation system and prove that taking into account redundant primary estimates such as sum of range measurements between the object of location and a pair of transceiver stations could improve single range accuracy estimation after joint processing with appropriate weighting coefficients. The approach for experimental evaluation is a testbed including four SDR-based transceiver stations, three of which perform primary measurements collection and one acts as the object of location estimation and measurement processing unit. Transceiver stations are working on National Instruments (NI) Universal Software Radio Peripheral (USRP) hardware with LabVIEW software, performing transmission, reception and processing of signals. Experiment was conducted in mobile scenario with slow pedestrian object of location movement and revealed position Mean Square Error (MSE) of one meter for range measurements with ten trial results accumulation.**

***Keyword*— Analytical model, Distance measurement, Radar signal processing, Radio navigation, Software radio**

I. INTRODUCTION

THE field of application of presented results are navigation, radar and sonar systems which consist of multiple transceiver stations gathering measurements, object of location estimation and measurement processing unit.

Increasing positioning accuracy is an important task for radio navigation systems in civil and military applications to accurately locate an aircraft or vehicle [1-3].

One of the ways for such flight tracking are MLAT systems widely developed in several countries. Its construction, navigation signals processing principles, base transceiver station synchronization approaches, functionality and operating modes are defined by conditions of practical application such as accuracy demands and location area topography [4].

Examples of widely spread Automatic Dependent Surveillance – Broadcast (ADS–B) multilateration radio navigation systems employed in aircraft navigation are presented in [5,6].

Multilateration navigation technique is based on TDOA (Time Difference of Arrival) measurements gathered by a number of ground base transceiver stations, which are placed in known locations and cover surrounding airspace. Time of Arrival (TOA) based algorithms and its comparison with TDOA are presented in [7]. Influence of geometric arrangement of base transceiver stations in conjunction with radio wave propagation conditions on the positioning accuracy by means of computer simulation and experimental validation is evaluated in [8]. Dependence of the base transceiver stations number and its geometric arrangement on the positioning accuracy is developed in [9]. Joint processing of range measurements in multilateration radio navigation system is investigated [10] and [11], however these work lack of experimental evaluation in field conditions. Experimental validation of multipoint joint processing of primary range measurement via software-defined radio (SDR) testbed is performed in [12].

The aim of this paper is to evolve the approach of analytical and experimental evaluation proposed in [12] and validate joint processing of primary range measurement algorithms influence on positioning accuracy in field conditions with slow pedestrian object of location movement.

The material in the paper is organized in the following order. Multipoint radio system under consideration, algorithm for joint processing and its analytical accuracy performance evaluation are presented in the second part. Developed software-defined radio MLAT, including experimental scenario and its accuracy performance evaluation results are presented in the third part. Finally, we draw the conclusions in the fourth part.

Manuscript received on November 15, 2016. This work was supported by Ministry of Science and Education of the Russian Federation within the scope of Federal Target Program «Research and development in priority sectors of scientific and technical complex of Russian Federation in 2014-2020 years» within the project «The development of experimental model of multi-position fast deployment self-contained radar system ground infrastructure for landing aircraft on unprepared ground» (unique project identifier RFMEF160714X0057).

Georgy Mashkov is with the State University of Telecommunication, 22 Prospekt Bolshevikov, St. Petersburg, Russia (e-mail: MashkovGM@sut.ru).

Eugene Borisov is with the State University of Telecommunication, 22 Prospekt Bolshevikov, St. Petersburg, Russia (e-mail: kafedra@sut.ru).

Grigorii Fokin is with the State University of Telecommunication, 22 Prospekt Bolshevikov, St. Petersburg, Russia (corresponding author phone: 8 921 985 80 04; e-mail: grihafokin@gmail.com).

II. Analytical Results on Multipoint Joint Processing of Range Measurements

A. MLAT with Joint Processing of Range Measurements Operating Principle

Multipoint joint processing radio system under consideration operates in the following way. Transceiver stations transmit unique signals based on pseudorandom binary sequence and then receive their retransmitted copies from object of location and thus gather time of arrival (TOA). Object of location estimation is an active reflector which retransmits unique signals. Finally measurement processing unit gathers TOA measurements from transceiver stations and derives range estimates between transceiver stations and object of location and after that performs joint processing of derived ranges to locate the object in a three-dimensional space based on known transceiver stations reference positions.

B. Joint Processing of Range Measurements Problem Statement

In general case MLAT joint processing of range measurements problem statement is formulated as follows. We assume that it includes N transceiver stations for gathering of measurements and so we get N possible range measurements between transceiver stations and object of location denoted by $R_1, R_2, ...R_N$ and $N(N-1)$ sum of range measurements denoted by $R_{\Sigma 12}, R_{\Sigma 21}, ...R_{\Sigma N(N-1)}$.

Algorithm for joint processing of range measurements was presented in prior work [12] that's why here we only rewrite main equations and notations.

It is a well-known fact, that system is redundant when $N \geq 3$ [10], that's why approach used for independent measurements acquisition enables us to form system of N^2 linear equations which is substantially redundant:

$$\begin{cases} \begin{cases} R_1 = 1 \cdot R_1 + 0 \cdot R_2 + 0 \cdot R_3 + ... + 0 \cdot R_N, \\ R_2 = 0 \cdot R_1 + 1 \cdot R_2 + 0 \cdot R_3 + ... + 0 \cdot R_N, \\ \vdots \\ R_1 = 0 \cdot R_1 + 0 \cdot R_2 + 0 \cdot R_3 + ... + 1 \cdot R_N, \end{cases} \\ \begin{cases} R_{\Sigma 12} = 1 \cdot R_1 + 1 \cdot R_2 + 0 \cdot R_3 + ... + 0 \cdot R_N, \\ R_{\Sigma 21} = 1 \cdot R_1 + 1 \cdot R_2 + 0 \cdot R_3 + ... + 0 \cdot R_N, \\ R_{\Sigma 13} = 1 \cdot R_1 + 0 \cdot R_2 + 1 \cdot R_3 + ... + 0 \cdot R_N, \\ R_{\Sigma 31} = 1 \cdot R_1 + 0 \cdot R_2 + 1 \cdot R_3 + ... + 0 \cdot \widetilde{R_N}, \\ \vdots \\ \widetilde{R_{\Sigma N}} = 1 \cdot \widetilde{R_1 + 0} \cdot \widetilde{R_2 + 0} \cdot \widetilde{R_3 + ...} + 1 \cdot \widetilde{R_N.} \end{cases} \end{cases} \quad (1)$$

In matrix form system of N^2 linear equations (1) can be represented as

$$\mathbf{H} = \mathbf{AS}, \quad (2)$$

where $\mathbf{H}^T = \left[R_1, R_2, ..., R_N, R_{\Sigma 12}, R_{\Sigma 21}, R_{\Sigma 13}, ..., R_{\Sigma N}\right]$ – row vector of range and sum of range measurements of size $1 \times N^2$; $\mathbf{A}$ – matrix of coefficients of size $N^2 \times N$, with elements equal to one for available in (1) range measurement and zero otherwise; $\mathbf{S}^T = \left[R_1, R_2, ..., R_N\right]$ – row vector of unknown range estimates of size $1 \times N$.

Solving (2) with nonlinear least squares estimation theory methods [11] we get the following solution:

$$\mathbf{S} = \left[\left(\mathbf{A}^T \mathbf{\Lambda} \mathbf{W}^{-1} \mathbf{A}\right)^{-1} \mathbf{A}^T \mathbf{\Lambda} \mathbf{W}^{-1}\right] \mathbf{H}, \quad (3)$$

where $\mathbf{W}$ – square matrix of primary range measurements accuracy of size $N^2 \times N^2$, with range and sum of range primary measurement error variance $\sigma^2_{R1}, \sigma^2_{R2}, ..., \sigma^2_{R\Sigma N}$ as diagonal elements, and possible correlations between them as non-diagonal elements:

$$\mathbf{W} = \begin{bmatrix} \sigma^2_{R1} & \cdots & \cdots & \cdots \\ \vdots & \sigma^2_{R1} & & \vdots \\ \vdots & & & \vdots \\ \cdots & \cdots & \cdots & \sigma^2_{R\Sigma_{N^2}} \end{bmatrix}, \quad (4)$$

$\mathbf{\Lambda}$ – diagonal matrix of coefficients j of size $N^2 \times N^2$ with diagonal elements equal to one for available in (1) range measurement and zero otherwise:

$$\mathbf{\Lambda} = \begin{bmatrix} j & 0 & 0 & 0 \\ 0 & j & 0 & 0 \\ 0 & 0 & & \vdots \\ 0 & 0 & \cdots & j \end{bmatrix}. \quad (5)$$

Geometric arrangement of MLAT under consideration is depicted in Fig. 1.

Multipoint range measurement radio system depicted in Fig. 1 has 3 spatially distributed transceiver stations with known reference positions in a three-dimensional space $(x_1, y_1, h_1), (x_2, y_2, h_2), (x_3, y_3, h_3)$ for gathering of range measurements R_1, R_2, R_3 between them and object of location.

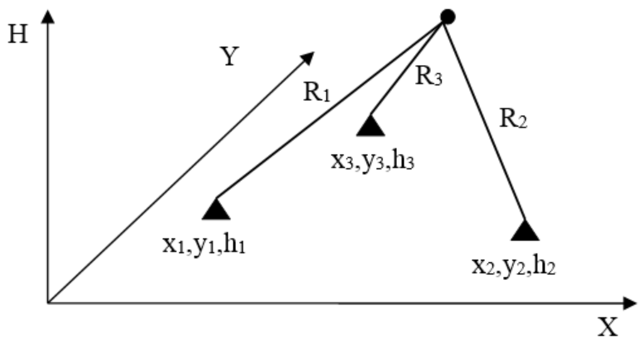

Fig. 1. MLAT radio navigation system with 3 transceiver stations

Developing an approach in [12] and taking into account range and sum of range primary measurement error variance equal to $\sigma_{R1}^2=\sigma_{R2}^2=\sigma_R^2$ and $\sigma_{R\Sigma12}^2=\sigma_{R\Sigma21}^2=\sigma_{R\Sigma}^2$ respectively, we can get following analytical solutions for unknown range estimates:

$$\begin{aligned}
\mathrm{R}_1 ={}& \frac{\mathrm{R}_1\left(\sigma_{\mathrm{R\Sigma}}^4+6\sigma_{\mathrm{R}}^2\sigma_{\mathrm{R\Sigma}}^2\right)}{\left(2\sigma_{\mathrm{R}}^2+\sigma_{\mathrm{R\Sigma}}^2\right)\left(8\sigma_{\mathrm{R}}^2+\sigma_{\mathrm{R\Sigma}}^2\right)}-\frac{2\mathrm{R}_2\sigma_{\mathrm{R}}^2\sigma_{\mathrm{R\Sigma}}^2}{\left(2\sigma_{\mathrm{R}}^2+\sigma_{\mathrm{R\Sigma}}^2\right)\left(8\sigma_{\mathrm{R}}^2+\sigma_{\mathrm{R\Sigma}}^2\right)}-\\
&-\frac{2\mathrm{R}_3\sigma_{\mathrm{R}}^2\sigma_{\mathrm{R\Sigma}}^2}{\left(2\sigma_{\mathrm{R}}^2+\sigma_{\mathrm{R\Sigma}}^2\right)\left(8\sigma_{\mathrm{R}}^2+\sigma_{\mathrm{R\Sigma}}^2\right)}+\frac{\mathrm{R}_{\Sigma12}\left(4\sigma_{\mathrm{R}}^2+\sigma_{\mathrm{R}}^2\sigma_{\mathrm{R\Sigma}}^2\right)}{\left(2\sigma_{\mathrm{R}}^2+\sigma_{\mathrm{R\Sigma}}^2\right)\left(8\sigma_{\mathrm{R}}^2+\sigma_{\mathrm{R\Sigma}}^2\right)}+\\
&+\frac{\mathrm{R}_{\Sigma21}\left(4\sigma_{\mathrm{R}}^2+\sigma_{\mathrm{R}}^2\sigma_{\mathrm{R\Sigma}}^2\right)}{\left(2\sigma_{\mathrm{R}}^2+\sigma_{\mathrm{R\Sigma}}^2\right)\left(8\sigma_{\mathrm{R}}^2+\sigma_{\mathrm{R\Sigma}}^2\right)}+\frac{\mathrm{R}_{\Sigma13}\left(4\sigma_{\mathrm{R}}^2+\sigma_{\mathrm{R}}^2\sigma_{\mathrm{R\Sigma}}^2\right)}{\left(2\sigma_{\mathrm{R}}^2+\sigma_{\mathrm{R\Sigma}}^2\right)\left(8\sigma_{\mathrm{R}}^2+\sigma_{\mathrm{R\Sigma}}^2\right)}+\\
&+\frac{\widehat{\mathrm{R}_{\Sigma31}}\left(4\sigma_{\mathrm{R}}^2+\sigma_{\mathrm{R}}^2\sigma_{\mathrm{R\Sigma}}^2\right)}{\left(2\sigma_{\mathrm{R}}^2+\sigma_{\mathrm{R\Sigma}}^2\right)\left(8\sigma_{\mathrm{R}}^2+\sigma_{\mathrm{R\Sigma}}^2\right)}-\frac{\widehat{\mathrm{R}_{\Sigma23}}\left(4\sigma_{\mathrm{R}}^2+\sigma_{\mathrm{R}}^2\sigma_{\mathrm{R\Sigma}}^2\right)}{\left(2\sigma_{\mathrm{R}}^2+\sigma_{\mathrm{R\Sigma}}^2\right)\left(8\sigma_{\mathrm{R}}^2+\sigma_{\mathrm{R\Sigma}}^2\right)}-\\
&-\frac{\widehat{\mathrm{R}_{\Sigma32}}\left(4\sigma_{\mathrm{R}}^2+\sigma_{\mathrm{R}}^2\sigma_{\mathrm{R\Sigma}}^2\right)}{\left(2\sigma_{\mathrm{R}}^2+\sigma_{\mathrm{R\Sigma}}^2\right)\left(8\sigma_{\mathrm{R}}^2+\sigma_{\mathrm{R\Sigma}}^2\right)},
\end{aligned} \tag{6}$$

$$\begin{aligned}
\mathrm{R}_2 ={}& \frac{2\mathrm{R}_1\sigma_{\mathrm{R}}^2\sigma_{\mathrm{R\Sigma}}^2}{\left(2\sigma_{\mathrm{R}}^2+\sigma_{\mathrm{R\Sigma}}^2\right)\left(8\sigma_{\mathrm{R}}^2+\sigma_{\mathrm{R\Sigma}}^2\right)}-\frac{\mathrm{R}_2\left(\sigma_{\mathrm{R\Sigma}}^4+6\sigma_{\mathrm{R}}^2\sigma_{\mathrm{R\Sigma}}^2\right)}{\left(2\sigma_{\mathrm{R}}^2+\sigma_{\mathrm{R\Sigma}}^2\right)\left(8\sigma_{\mathrm{R}}^2+\sigma_{\mathrm{R\Sigma}}^2\right)}-\\
&-\frac{2\mathrm{R}_3\sigma_{\mathrm{R}}^2\sigma_{\mathrm{R\Sigma}}^2}{\left(2\sigma_{\mathrm{R}}^2+\sigma_{\mathrm{R\Sigma}}^2\right)\left(8\sigma_{\mathrm{R}}^2+\sigma_{\mathrm{R\Sigma}}^2\right)}+\frac{\mathrm{R}_{\Sigma12}\left(4\sigma_{\mathrm{R}}^2+\sigma_{\mathrm{R}}^2\sigma_{\mathrm{R\Sigma}}^2\right)}{\left(2\sigma_{\mathrm{R}}^2+\sigma_{\mathrm{R\Sigma}}^2\right)\left(8\sigma_{\mathrm{R}}^2+\sigma_{\mathrm{R\Sigma}}^2\right)}+\\
&+\frac{\mathrm{R}_{\Sigma21}\left(4\sigma_{\mathrm{R}}^2+\sigma_{\mathrm{R}}^2\sigma_{\mathrm{R\Sigma}}^2\right)}{\left(2\sigma_{\mathrm{R}}^2+\sigma_{\mathrm{R\Sigma}}^2\right)\left(8\sigma_{\mathrm{R}}^2+\sigma_{\mathrm{R\Sigma}}^2\right)}-\frac{\mathrm{R}_{\Sigma13}4\sigma_{\mathrm{R}}^4}{\left(2\sigma_{\mathrm{R}}^2+\sigma_{\mathrm{R\Sigma}}^2\right)\left(8\sigma_{\mathrm{R}}^2+\sigma_{\mathrm{R\Sigma}}^2\right)}+\\
&-\frac{4\mathrm{R}_{\Sigma31}\sigma_{\mathrm{R}}^4}{\left(2\sigma_{\mathrm{R}}^2+\sigma_{\mathrm{R\Sigma}}^2\right)\left(8\sigma_{\mathrm{R}}^2+\sigma_{\mathrm{R\Sigma}}^2\right)}+\frac{\widehat{\mathrm{R}_{\Sigma23}}\left(4\sigma_{\mathrm{R}}^2+\sigma_{\mathrm{R}}^2\sigma_{\mathrm{R\Sigma}}^2\right)}{\left(2\sigma_{\mathrm{R}}^2+\sigma_{\mathrm{R\Sigma}}^2\right)\left(8\sigma_{\mathrm{R}}^2+\sigma_{\mathrm{R\Sigma}}^2\right)}-\\
&-\frac{\widehat{\mathrm{R}_{\Sigma32}}\left(4\sigma_{\mathrm{R}}^2+\sigma_{\mathrm{R}}^2\sigma_{\mathrm{R\Sigma}}^2\right)}{\left(2\sigma_{\mathrm{R}}^2+\sigma_{\mathrm{R\Sigma}}^2\right)\left(8\sigma_{\mathrm{R}}^2+\sigma_{\mathrm{R\Sigma}}^2\right)},
\end{aligned} \tag{7}$$

$$\begin{aligned}
\mathrm{R}_3 ={}& \frac{2\mathrm{R}_1\sigma_{\mathrm{R}}^2\sigma_{\mathrm{R\Sigma}}^2}{\left(2\sigma_{\mathrm{R}}^2+\sigma_{\mathrm{R\Sigma}}^2\right)\left(8\sigma_{\mathrm{R}}^2+\sigma_{\mathrm{R\Sigma}}^2\right)}-\frac{2\mathrm{R}_2\sigma_{\mathrm{R}}^2\sigma_{\mathrm{R\Sigma}}^2}{\left(2\sigma_{\mathrm{R}}^2+\sigma_{\mathrm{R\Sigma}}^2\right)\left(8\sigma_{\mathrm{R}}^2+\sigma_{\mathrm{R\Sigma}}^2\right)}+\\
&+\frac{\mathrm{R}_3\left(\sigma_{\mathrm{R\Sigma}}^4+6\sigma_{\mathrm{R}}^2\sigma_{\mathrm{R\Sigma}}^2\right)}{\left(2\sigma_{\mathrm{R}}^2+\sigma_{\mathrm{R\Sigma}}^2\right)\left(8\sigma_{\mathrm{R}}^2+\sigma_{\mathrm{R\Sigma}}^2\right)}-\frac{4\mathrm{R}_{\Sigma12}\sigma_{\mathrm{R}}^4}{\left(2\sigma_{\mathrm{R}}^2+\sigma_{\mathrm{R\Sigma}}^2\right)\left(8\sigma_{\mathrm{R}}^2+\sigma_{\mathrm{R\Sigma}}^2\right)}-\\
&-\frac{4\mathrm{R}_{\Sigma21}\sigma_{\mathrm{R}}^4}{\left(2\sigma_{\mathrm{R}}^2+\sigma_{\mathrm{R\Sigma}}^2\right)\left(8\sigma_{\mathrm{R}}^2+\sigma_{\mathrm{R\Sigma}}^2\right)}-\frac{\mathrm{R}_{\Sigma13}\left(4\sigma_{\mathrm{R}}^2+\sigma_{\mathrm{R}}^2\sigma_{\mathrm{R\Sigma}}^2\right)}{\left(2\sigma_{\mathrm{R}}^2+\sigma_{\mathrm{R\Sigma}}^2\right)\left(8\sigma_{\mathrm{R}}^2+\sigma_{\mathrm{R\Sigma}}^2\right)}-\\
&-\frac{\mathrm{R}_{\Sigma31}\left(4\sigma_{\mathrm{R}}^2+\sigma_{\mathrm{R}}^2\sigma_{\mathrm{R\Sigma}}^2\right)}{\left(2\sigma_{\mathrm{R}}^2+\sigma_{\mathrm{R\Sigma}}^2\right)\left(8\sigma_{\mathrm{R}}^2+\sigma_{\mathrm{R\Sigma}}^2\right)}+\frac{\widehat{\mathrm{R}_{\Sigma23}}\left(4\sigma_{\mathrm{R}}^2+\sigma_{\mathrm{R}}^2\sigma_{\mathrm{R\Sigma}}^2\right)}{\left(2\sigma_{\mathrm{R}}^2+\sigma_{\mathrm{R\Sigma}}^2\right)\left(8\sigma_{\mathrm{R}}^2+\sigma_{\mathrm{R\Sigma}}^2\right)}-\\
&-\frac{\widehat{\mathrm{R}_{\Sigma32}}\left(4\sigma_{\mathrm{R}}^2+\sigma_{\mathrm{R}}^2\sigma_{\mathrm{R\Sigma}}^2\right)}{\left(2\sigma_{\mathrm{R}}^2+\sigma_{\mathrm{R\Sigma}}^2\right)\left(8\sigma_{\mathrm{R}}^2+\sigma_{\mathrm{R\Sigma}}^2\right)}.
\end{aligned} \tag{8}$$

C. Joint Processing Range Estimates Accuracy Analysis

Equations (6) – (8) are range estimates between transceiver stations and object of location derived by measurement processing unit from primary range measurements received from all transceiver stations. Let's define range estimates variance as $\sigma_{\mathrm{RK}}^{2}=\mathrm{diag}\left(\mathbf{A}^{\mathrm{T}}\mathbf{W}^{-1}\mathbf{A}\right)^{-1}$, then computed range estimates variance for (6) – (8) can be expressed by

$$\sigma_{\mathrm{RK}}^{2}=\frac{\sigma_{\mathrm{R}}^2}{16\sigma_{\mathrm{R}}^4+10\sigma_{\mathrm{R}}^2\sigma_{\mathrm{R\Sigma}}^2+\sigma_{\mathrm{R\Sigma}}^4}\cdot\begin{bmatrix}6\sigma_{\mathrm{R}}^4\sigma_{\mathrm{R\Sigma}}^2+\sigma_{\mathrm{R}}^2\sigma_{\mathrm{R\Sigma}}^4 & -2\sigma_{\mathrm{R}}^4\sigma_{\mathrm{R\Sigma}}^2 & -2\sigma_{\mathrm{R}}^4\sigma_{\mathrm{R\Sigma}}^2\\ -2\sigma_{\mathrm{R}}^4\sigma_{\mathrm{R\Sigma}}^2 & 6\sigma_{\mathrm{R}}^4\sigma_{\mathrm{R\Sigma}}^2+\sigma_{\mathrm{R}}^2\sigma_{\mathrm{R\Sigma}}^4 & -2\sigma_{\mathrm{R}}^4\sigma_{\mathrm{R\Sigma}}^2\\ -2\sigma_{\mathrm{R}}^4\sigma_{\mathrm{R\Sigma}}^2 & -2\sigma_{\mathrm{R}}^4\sigma_{\mathrm{R\Sigma}}^2 & 6\sigma_{\mathrm{R}}^4\sigma_{\mathrm{R\Sigma}}^2+\sigma_{\mathrm{R}}^2\sigma_{\mathrm{R\Sigma}}^4\end{bmatrix}. \tag{9}$$

Replacing range and sum of range primary measurement error variance in (6) – (8) by range estimate variances computed beforehand, we can get optimal estimation algorithm for range estimation in the case of unknown error variances.

It can be shown that

$$\lim_{\sigma_{\mathrm{R}}\to\infty}\left(\mathbf{A}^{\mathrm{T}}\mathbf{W}^{-1}\mathbf{A}\right)^{-1}=\frac{1}{8}\begin{bmatrix}3 & -1 & -1\\ -1 & 3 & -1\\ -1 & -1 & 3\end{bmatrix}\sigma_{\mathrm{R\Sigma}}^2, \tag{10}$$

$$\lim_{\sigma_{\mathrm{R\Sigma}}\to\infty}\left(\mathbf{A}^{\mathrm{T}}\mathbf{W}^{-1}\mathbf{A}\right)^{-1}=\begin{bmatrix}1 & 0 & 0\\ 0 & 1 & 0\\ 0 & 0 & 1\end{bmatrix}\sigma_{\mathrm{R}}^2, \tag{11}$$

$$\lim_{\sigma_{\mathrm{R}}\to\sigma_{\mathrm{R\Sigma}}}\left(\mathbf{A}^{\mathrm{T}}\mathbf{W}^{-1}\mathbf{A}\right)^{-1}=\frac{1}{27}\begin{bmatrix}7 & -2 & -2\\ -2 & 7 & -2\\ -2 & -2 & 7\end{bmatrix}\sigma_{\mathrm{R\Sigma}}^2, \tag{12}$$

$$\lim_{\sigma_{\mathrm{R\Sigma}}\to\sigma_{\mathrm{R}}}\left(\mathbf{A}^{\mathrm{T}}\mathbf{W}^{-1}\mathbf{A}\right)^{-1}=\frac{1}{27}\begin{bmatrix}7 & -2 & -2\\ -2 & 7 & -2\\ -2 & -2 & 7\end{bmatrix}\sigma_{\mathrm{R}}^2, \tag{13}$$

$$\lim_{\sigma_{\mathrm{R}}\to 0}\left(\mathbf{A}^{\mathrm{T}}\mathbf{W}^{-1}\mathbf{A}\right)^{-1}=0,\ \lim_{\sigma_{\mathrm{R\Sigma}}\to 0}\left(\mathbf{A}^{\mathrm{T}}\mathbf{W}^{-1}\mathbf{A}\right)^{-1}=0\,. \tag{14}$$

From the analysis of (10) – (14) we can conclude that increasing range and sum of range primary measurement error variance to maximum does not affect correct joint processing algorithm operation hence it is possible to increase range estimation accuracy by primary redundant measurement trials accumulation [12].

III. Experimental Results on MLAT with Joint Processing of Range Measurements

A. Developed Software-Defined Radio MLAT Testbed

To realize experimental validation of proposed algorithm for multipoint joint processing of range measurements with trial results accumulation we developed a software-defined radio MLAT testbed by means of model based design via software defined radio [14] on National Instruments hardware NI USRP-2932 [15] and LabVIEW software [16]. It consists of three transceiver stations gathering measurements, one transceiver station realizing functions of an object of location (active reflector), and one processing unit. Layout of the developed multipoint software-defined radio testbed for joint processing of range measurements experimental evaluation is depicted in Fig. 2.

NI USRP-2932 worked in 433 MHz Low Power Devices (LPD) band with power constraint of 20 dBm for communication with binary phase shift keying signals of 2 MHz bandwidth modulated by unique pseudorandom Gold sequence with 500 ns pulse duration and 3 ms pulse-repetition cycle.

It is worth noting, that previous experimental validation [12] was carried out for indoor laboratory conditions in the static scenario when transceiver stations and object of location were placed in the room with spatial separation of several decades of meters and worked stationary. To ensure autonomous mobile deployment for outdoor field conditions of presented MLAT testbed we manufactured 4 prototype models of transceiver stations with self-contained power supply and cooling depicted in Fig. 3.

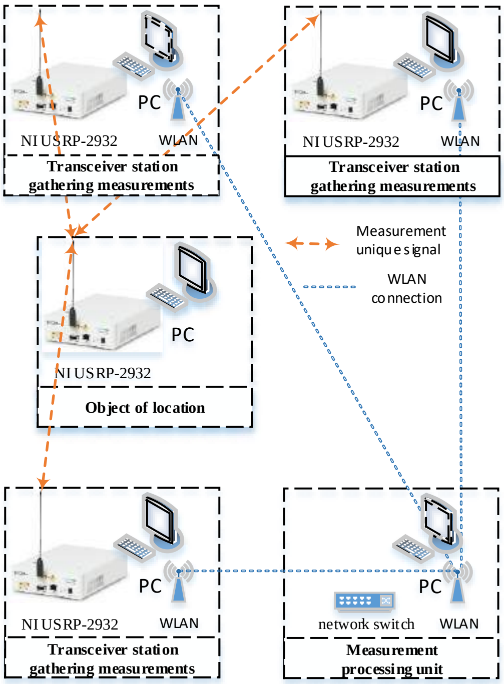

Fig. 2. MLAT radio navigation system with 3 transceiver stations

Fig. 3. Prototype of mobile autonomous manufactured MLAT transceiver station

Transceiver stations are realized on National Instruments hardware NI USRP-2932 and work under specially developed LabVIEW software applications. Developed software-defined radio testbed operates in the following way [12]. Transceiver stations based on NI USRP-2932 and working on Core I7 microPC under Windows 7 with LabVIEW application “Server” transmit unique signals based on pseudorandom binary sequence and then receive their retransmitted copies from object of location and thus gather TOA. Object of location estimation is an active reflector based on NI USRP-2932 and working on Core I7 microPC under Windows 7 with LabVIEW application “Repeater” which retransmits unique signals, received from “Server”. Finally, measurement processing unit working on Core I7 microPC under Windows 7 with LabVIEW application “Active Positioning” gathers multiple TOA primary measurements from transceiver stations, process them and visualize result.

To provide investigation of positioning accuracy for outdoor mobile conditions we mounted manufactured transceiver stations and antennas on carts with slow pedestrian object of location movement capability as depicted in Fig. 4.

We used 2 omnidirectional antennas AH-433: one for transmit and one for receive channel as depicted in Fig. 5.

Fig. 4. Mobile organization of experiment layout

Fig. 5. Antenna AH-433

B. *Experimental Scenario and its Accuracy Performance Evaluation Results*

Experiment was carried out in the court of the Bonch-Bruevich St. Petersburg State University of

Telecommunications with object of location track movement according to layout, depicted in Fig. 6.

During experiment 3 manufactured MLAT transceiver stations operated in the mode of gathering primary measurements and one transceiver station operated as the object of location and measurement processing unit with spatial separation of several decades of meters under line of sight (LOS) conditions.

Network connection between transceiver stations gathering primary measurements and processing unit is based on IEEE 802.11n WLAN. Estimated positioning accuracy was visualized in the LabVIEW application “Active Positioning” running on measurement processing unit and true ranges were estimated by laser ranger.

We performed positioning accuracy performance evaluation in terms of range measurements MSE for two cases of joint processing: with and without primary redundant measurement trials accumulation. During experimental evaluation we got following results in terms of MSE depicted in Fig. 7 and Fig. 8.

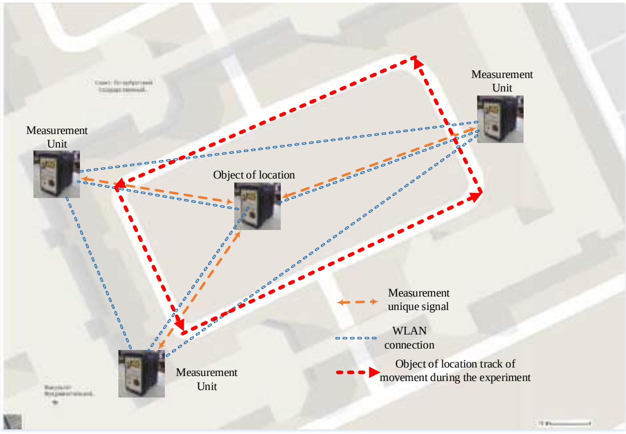

Fig. 6. Experiment layout in the court of The Bonch-Bruevich St. Petersburg State University of Telecommunications

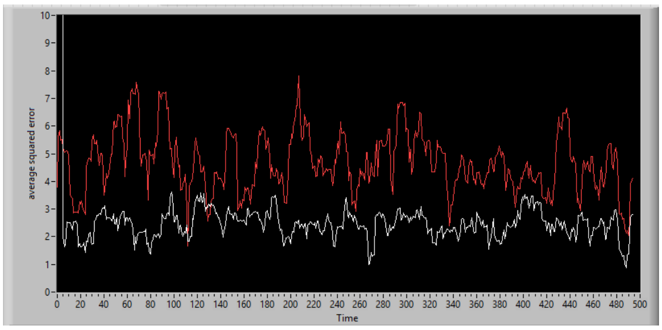

Fig. 7. MSE for range measurements without trial results accumulation

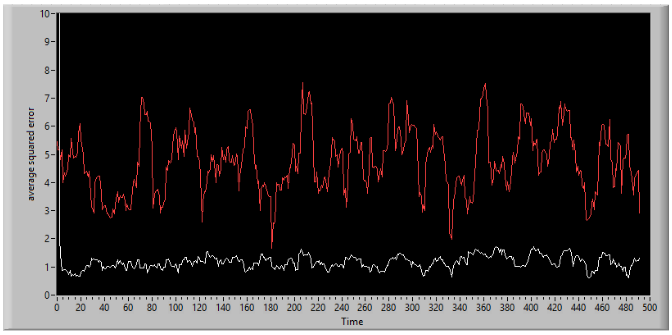

Fig. 8. MSE for range measurements with ten trial results accumulation

We have the following notations in Fig. 7 and Fig. 8 considering experimental evaluation in terms of MSE: upper (red) line indicates range and sum of range primary measurement error variance and lower (white) line indicates range estimation error variance after joint processing over time in the steady-state condition; Fig. 7 demonstrates the range MSE in meters for the case without trial results accumulation while Fig. 8 demonstrates range MSE in meters for the case of joint processing and ten trial results accumulation. It can be seen, that increasing the number of trial results accumulation during joint processing can double positioning accuracy estimation in terms of MSE up to one meter and these field results confirm the result reported in [12] for laboratory testbed evaluation.

IV. Conclusion

In the conclusion we can state that joint processing of range measurements with trial results accumulation can double positioning accuracy and approach MSE of one meter. An algorithm for such processing was proposed, then it was evaluated analytically and finally it was experimentally validated with software-defined radio testbed specially manufactured for outdoor mobile conditions.

References

[1] V. Averianov, Multiposition radar station and system. *Science and Technics, Minsk*, 1978.
[2] V.S. Chernyak, The multiposition radar. *Radio and Communications, Moscow*, 1993.
[3] V.S. Chernyak, Fundamentals of Multisite Radar System. *Gordon and Breach Science Publishers*, 1998.
[4] ICAO: Multilateration (MLAT) Concept of Use, 2007.
[5] ERA company. (2015, February 27). NEO datasheet. [Online]. Available: http://www.era.cz/downloads/data-sheets/NEO.pdf
[6] ICAO organization. (2011, September 2). ADSB, WAM, MLAT ATM International & Airports ADSB, WAM, MLAT implementations. ADSB/WAM integration Systems. [Online]. Available: http://www.icao.int/NACC/Documents/Meetings/2011/ADSBMLT/Day01-04-INDRA-INDRA.pdf
[7] M. Leonardi, A. Mathias, G. Galati, “Closed form localization algorithms for mode S wide area multilateration”, *in Radar Conference*, pp. 73-76, EuRAD, 2009.
[8] J. Honda, Y. Kakubari, T. Koga, “DOP simulation considering LOS/NLOS for aircraft positioning on airport surface”, *in: IEEE 5th Asia-Pacific Conference on Synthetic Aperture Radar (APSAR)*, pp. 773-776, 2015.
[9] P. Xinxin, L. Yong, L. Wei, Z. Yanbo, W. Yongchun, “An approach of fast stations selection algorithm for multilateration surveillance system”, *in Integrated Communications, Navigation and Surveilance Conference (ICNS)*, pp. P1-1-P1-7. Herndon, VA, 2011.
[10] G.M. Mashkov, E.G. Borisov, A.G. Vladyko, A.I. Gomonova, “The Use of Software-Defined Radio Systems in Multilateral Navigation Radio Systems”, *Infocommunications Journal*, vol. VII. n. 2. pp. 26-31, 2015.
[11] E.G. Borisov, G. M. Mashkov, A. G. Vladyko, “Analysis of Object Positioning Accuracy Provided by Range-Finding Systems of Various Types”, *Russian Aeronautics*. Vol. 58 № 4. pp. 401-406, 2015.
[12] E. Borisov, G. Mashkov, G. Fokin, “Experimental Validation of Multipoint Joint Pro-cessing of Range Measurements via Software-Defined Radio Testbed*”, in: 18th International Conference on Advanced Communication Technology (ICACT)*, pp.268-273, 2016.
[13] E.G. Borisov, S.V. Bachevskiy, G. M. Mashkov, “Increasing Estimation Accuracy of Unknown Parameters by Means of Cooperative Processing of Redundant Measurements in a System of Spatially Distributed Sensors”, *Sensors an Systems*. № 12 (198). pp.16-20, 2015.

[14] G.A. Fokin, D.V. Bulanov, D.B. Volgushev, “Radio communication systems model based design via software defined radio”, *Vestnik sviazy*, vol. 6, pp. 26-31, 2015.
[15] National Instruments company. (2015, August 17). NI USRP-292x/293x datasheet. Universal Software Radio Peripherals. [Online]. Available: http://www.ni.com/datasheet/pdf/en/ds-355
[16] LabVIEW home page. [Online]. Available: http://www.labview.ru/

Georgiy Mashkov was born in 1954 in Uzlovaya, a town and the administrative center of Uzlovsky District in Moscow Region. He graduated Kiev Higher engineering school in 1977 as the engineer at speciality air defence systems, then received Ph. D and D. Sc there in 1984 and 1993 respectively.

He is working is working in St.Petersburg University of Telecommunication as first Vice-rector (Vice rector for Academic Affairs). His studies focus on radio navigation.

Dr. Sc. Mashkov is Honorary Worker of Higher Professional Education of Russia.

Evgeny Borisov was born in 1967 in Novosibirsk. He graduated Kiev Higher engineering school in 1990 as the engineer at speciality air defence systems, then received Ph. D in 2000 in Smolensk Higher engineering school.

He is working is working in St.Petersburg University of Telecommunication as leading researcher of St.Petersburg University of Telecommunication.

Grogorii Fokin was born in 1984 in Pskov. He graduated St.Petersburg University of Telecommunication in 2005 as the engineer at speciality radiocommunications, then received Ph. D there in 2009.

He is working is working in St.Petersburg University of Telecommunication as Associate Professor of Department of Radio Communications and Signal Broadcasting..

Volume 6 Issue 1, Jan. 2017, ISSN: 2288-0003

ICACT-TACT
JOURNAL

GIRI Global IT Research Institute

1713 Obelisk, 216 Seohyunno, Bundang-gu, Sungnam Kyunggi-do, Republic of Korea 13591
Business Licence Number : 220-82-07506, Contact: secretariat@icact.org Tel: +82-70-4146-4991